Chapter 8

# Observation of the Rotor Position to Control the Synchronous Machine without Mechanical Sensor

## 8.1. State of the art

Intense industrialization has resulted in a large proliferation of electromechanical actuators in an increasing number of industries (home automation, transportation, heavy industry, etc.). More recently, this phenomenon has greatly affected embedded systems in which the electrical solution is preferred over the traditional hydraulic solution. This is due to the specificities of the electrical actuator, characterized by gains in power and mass volume, as well as to the many diagnosis and monitoring possibilities that this type of actuator facilitates. The embedded devices reveal a large number of actuators necessary for the movement control of different objects (servo-cylinders, electric pumps, windages, etc.). Specifications involve speed systems to follow and positioning trajectories to satisfy, paving the way for different and varied actuators obtaining different power and quality in the function finally obtained. We often find trapezoid electromotive force magnetic machines for speed control as well as sinusoidal electromotive force machines to ensure position control. Other combinations are clearly possible and thus a machine, developing trapezoid electromotive forces, can be fed by sinusoidal currents and vice versa.

---

Chapter written by Stéphane CAUX and Maurice FADEL

*Electrical Actuators: Identification and Observation* Edited by Bernard de Fornel and Jean-Paul Louis

Because of the increase in speed, often dictated by the goal of volume reduction, controlling these actuators creates new challenges directly affecting the nature of the algorithms used and organs necessary to the calculation. The switch frequency, often set in order to control switching losses and electromagnetic disturbances, should be great enough to impose correct waveshapes for currents, without penalizing real-time calculation devices. At this level, the low value of cyclic inductance creates serious problems. The correction chain is the subject of interest for the choice of modulator (Space Vector Modulation (SVM), regular symmetrical Pulse Width Modulation (PWM), etc.) for widening the zone of linearity of the inverter, as well as for the quality of measures where the accumulation of delays and/or the presence of noises can turn out to be harmful for accurate torque control. Global optimization of this methodology often goes through a reduction in the number of electric sensors (current, voltage). A significant evolution in terms of cost, volume, and reliability should obviously be obtained to get rid of the position sensor, that is, rebuilding the position from measured electric variables. We can witness here a reversal of the situation because even though the synchronous machine was highly developed, it is in large part because of the systematic use of the position sensor, ensuring a control of the rotor evolution and avoiding a machine stall. This constituted a challenge for many years, and the new challenge today consists of suppressing this sensor. Observation techniques are now operational, and this observation, associated with a startup procedure, can replace the collection device [VAS 01]. The reasons for which we want to get rid of the position sensor can be listed as follows:

– difficult atmosphere, not desirable for the sensor (drilling machine, embedded system, etc.);

– reduction of infinitely variable induction transmission cost (mass channel product, etc.);

– improvement of availability (limit the possibilities of mechanical failures, etc.);

– deletion of generally long operators in order to facilitate assembly (that is often the case for embedded systems in cars, etc.);

– reliable liberation of signal transmission problems between the sensor and control, especially over long distances.

Knowing the position of the rotor is vital to the self-piloted machine, that is, for the establishment of a link between the frequency of rotation and the feed frequency. However, following the structure of the machine, this position should be known in a continuous way, that is, with high resolution for sinusoidal current or discrete feed, with low resolution, for powering rectangular currents. These two objectives determine specific methods to observe the position, leading to different

developments [GAS 02]. Globally, and regardless of the type of machine, we can observe two approaches:

– the first approach by using electromotive forces (Figure 8.1). It has several solutions depending on the nature of the machine and its power supply type. With a machine fed by rectangular wave (Figure 8.1a), a phase is cyclically not connected and it becomes possible to measure the electromotive force produced by the machine. By combination, it is possible to build a synchronized signal on electromotive force harmonic 3 and guide the inverter switches. It is also possible to access electromotive forces with the help of an observer based on the measures of line currents and phase to ground or phase-to-phase voltage (Figure 8.1b). Following the nature of the machine used, we then have access to the position in a continuous way in one mechanical round or with synchronization signals spaced at electric 60°.

– the second approach, based on the reconstruction of position directly with the help of a looped model (Figure 8.2), considering or not the noises of measurements and using electric measures. There are many solutions for this course depending on the model of the machine used (abc, dq, $\alpha\beta$, ba-ca), accessible measurements (phase-to-ground voltage, phase-to-phase voltage, line currents, direct inverter voltage, etc.) or to the nature of the observer (Kalman filter, Luenberger observer, sliding mode observer, analytical redundancy observer, etc.).

These methods are generally powerful depending on operation zones (very slow speed, very high speed) as well as on the nature of parametric variations being undergone by the machine (evolution of mechanical or electric parameters). In fact, at high speed, it becomes difficult to make a lot of calculations because of increasing temporal constraints, and on the other hand, at low speed, the electromotive forces are very low and the information becomes difficult to extract.

Nevertheless, we should provide the method chosen with a device ensuring the startup of the machine. In fact, during startup, the rotor position is not known and the application of a voltage sequence can lead to a rotation in any axis. Although this phenomenon is not always a problem (cooling fan type application, etc.), it is often imperative to avoid it, and thus we should add to the method of position reconstruction a rotor blocking device or a localization procedure.

This last problem was the subject of a large number of publications in the last few years, notably in the case of smooth pole synchronous machines for which the solution is not necessarily trivial [KIM 03, SCH 03].

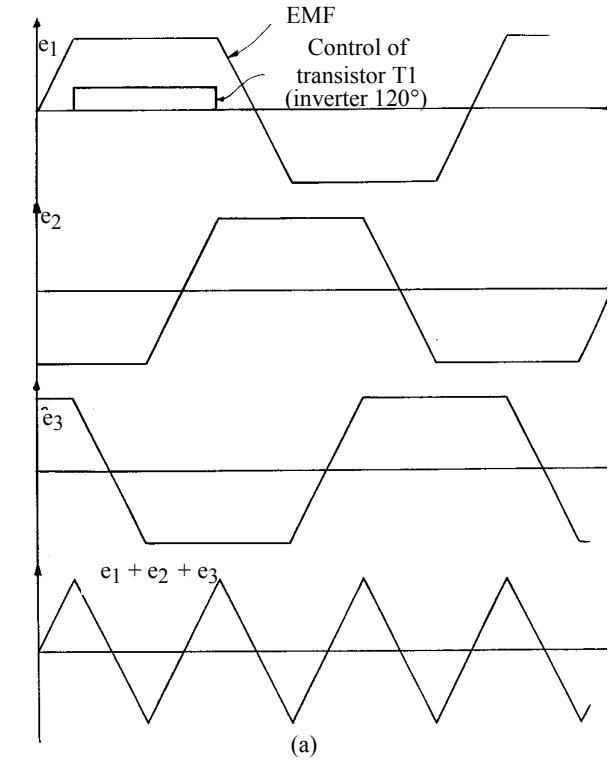


(a)

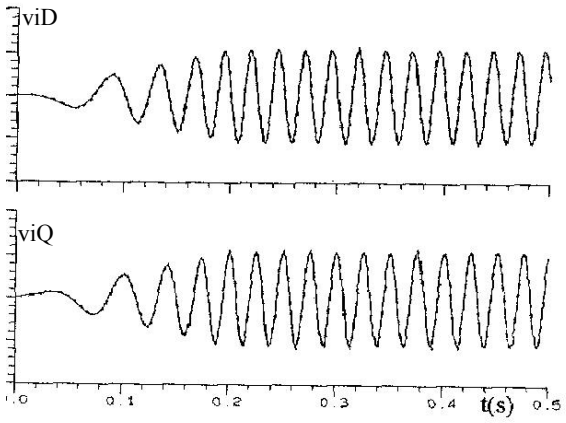


(b)

**Figure 8.1.** *Temporal feed signals (a) by rectangular currents; (b) by sinusoidal currents*

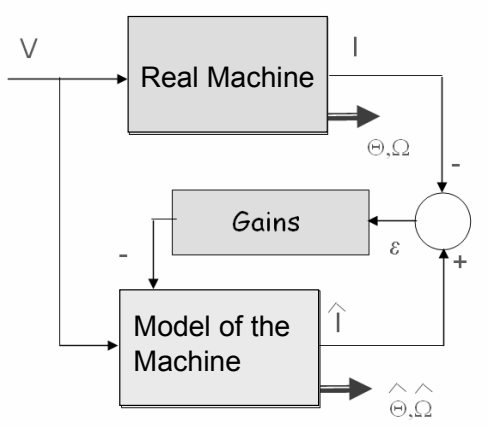


**Figure 8.2.** *Observation with the help of a reference model*

In fact, for salient pole machines, the structure of the rotor and especially the variation of cyclical inductances based on the rotor position can give us information. Through measurements of this inductance, or by the injection of signals and the analysis of corresponding harmonics, or by generating two-phase voltage sequences not generating a rotating field but generating position information, carrier currents are linked to these currents and positions of magnets [BOU 06, SCH 03].

The smooth pole synchronous machines, as the name indicates, do not have inductance variation, and values in direct axis and in quadrature are equal and constant. With blocked rotor, on the other hand, it is possible to inject voltage vectors to excite the saturation of the magnetic circuit that will be maximal or minimal in relation to magnets axis direction, for example [JEO 03]. Even though the application tolerates movement in pre-startup phase, the simplest solution consists of imposing a fixed voltage vector, and thus forcing a set magnetic vector during a certain duration. Time enough for the free rotor and its mechanic to be put in place and go from unknown startup to imposed position. The detection problem of the initial position would deserve a complete chapter and will no longer be discussed here.

## 8.2. Reconstruction of the low-resolution position

This procedure mainly involves the trapezoid electromotive force machines used in speed variation applications. In this case, the idea is to impose rectangular currents in phases (Figure 8.3). At every 60 electric degrees, we have to change the configuration of inverter switches to ensure the correct evolution of the machine.

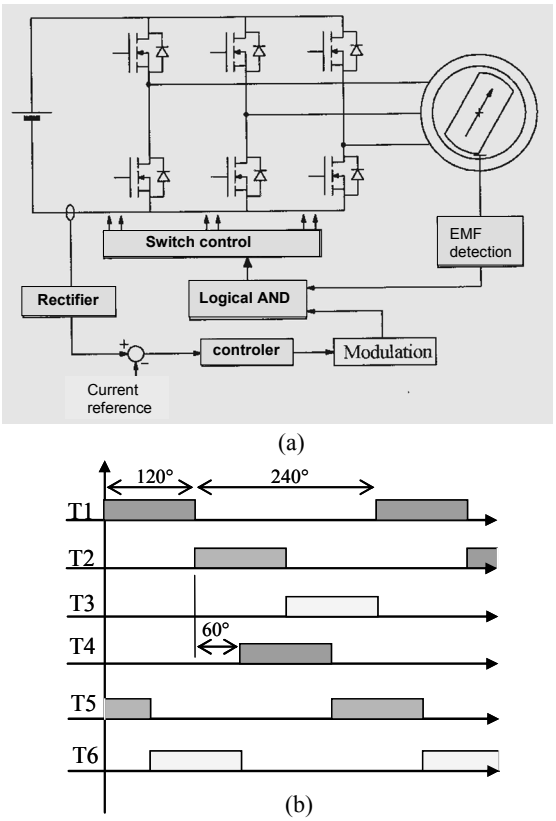


**Figure 8.3.** *(a) Variable synchronous speed drive; (b) semiconductors conduction intervals*

We should note that if electromotive forces are not sinusoidal, their sum is not zero and contribute to order 3. In this way, harmonic 3 is present and can be used to synchronize control orders. Several methods are thus based on the generation of the sum of electromotive forces [CAR 90].

### 8.2.1. *Equivalent electromotive force measure*

For trapezoid machines, where periodic knowledge of the position is sufficient, we can imagine devices generating a synchronization signal for the cyclical

imposition of appropriate currents with the rotor position. For each phase, we can write:

$$V_{s1}=R_{s1}.I_1+(L_s-M_s).\frac{dI_{s1}}{dt}+E_1 \qquad [8.1]$$

The reconstruction of electromotive force $E_1$ then involves the derivative of the stator current, which can be evaluated by placing a serial transformer (Figure 8.4). In fact, the secondary voltage of a transformer is linked to the derivative of the primary current.

This solution is certainly not in line with mass decrease, but it proposes a solution of integration and reliability that we should generally use for simple applications.

### 8.2.2. *Reconstruction of the sum of electromotive forces using the machine neutral*

By considering the three phases, we have:

$$V_{s1}+V_{s2}+V_{s3}=E_1+E_2+E_3 \qquad [8.2]$$

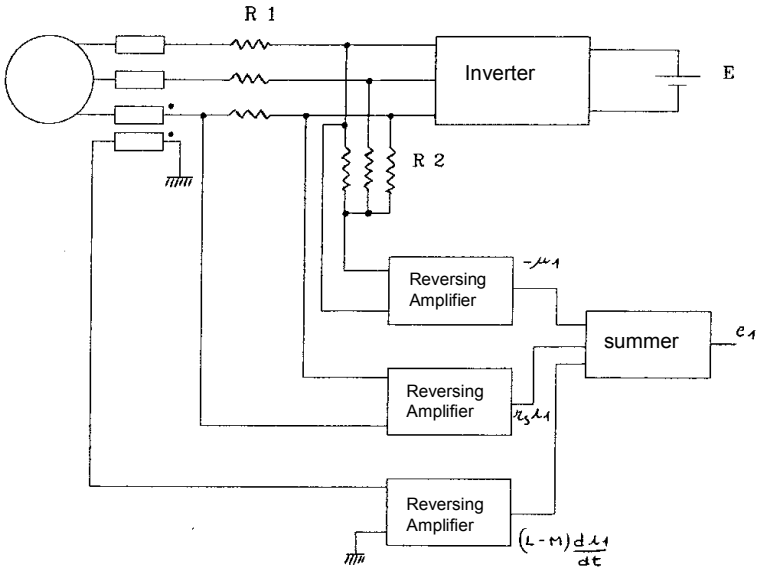


**Figure 8.4.** *Estimation of electromotive forces by current derivation by using a transformer*

Since the sum is not zero, the resulting signal can be used for controlling the synchronous machine.

If we can access the neutral point of the machine, we can control the machine with this signal (Figure 8.5).

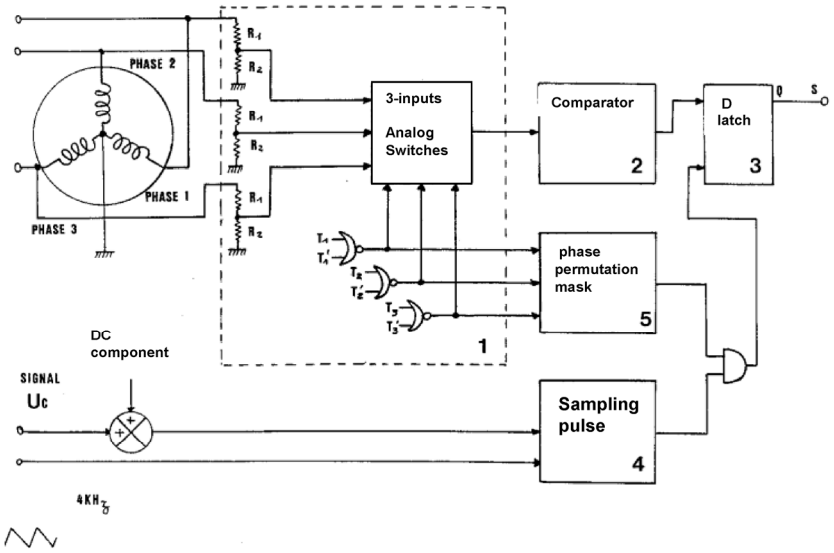


**Figure 8.5.** *Reconstruction of the sum of electromotive forces using the machine neutral*

We are in the field of specifically designed machines involving extra cost because of the need for an additional conductor. However, the efficiency and simplicity are present. It is necessary to be careful with filtering this signal, however, as it remains quite tainted by the commutations of the inverter (Figure 8.6).

### 8.2.3. *Use of the extended Park reference*

Trapezoid electromotive forces are part of non-sinusoidal electromotive force machines for which reference (d, q) modeling has very little interest. There is, however, a reference inwhich modeling retains its properties similar to the Park reference. This transformation [8.3] consists of rotating reference (α, β) not from the electric angle $\theta$ but from angle $\theta + \mu(\theta)$, where $\mu(\theta)$ aligns one of the

axes of the new reference with the vector representing the stator flux induced by the rotor [GRE 95].

$$V_{de}=R_s\cdot I_{de}+L\cdot\frac{dI_{de}}{dt}-\omega\cdot(1+\frac{d\mu}{d\theta})I_{qe}$$
$$V_{qe}=R_s\cdot I_{qe}+L\cdot\frac{dI_{qe}}{dt}+\omega\cdot(1+\frac{d\mu}{d\theta})I_{de}+\omega.\phi_r \qquad [8.3]$$

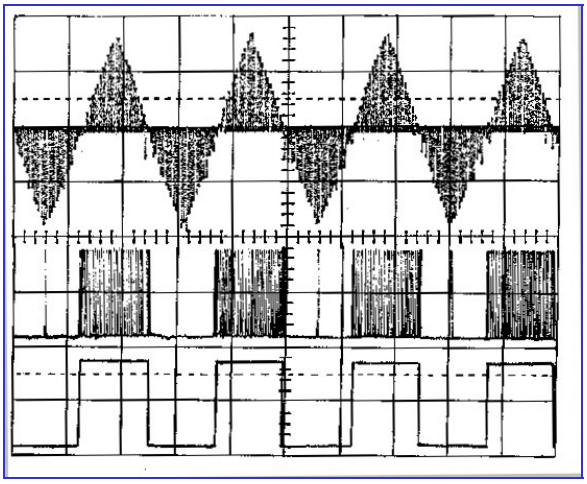

**Figure 8.6.** *Electromotive force sum and drive pulses*

In this extended Park reference, the model retains a certain number of properties identical to the traditional Park reference for sinusoidal electromotive force machines. For example, torque only depends on a component of the stator current. This can be used in control in order to minimize the losses because of Joule effect. The properties of this model make it possible to apply a few observation methods that will be seen in the case of sinusoidal electromotive force machines, such as the principle of analytical redundancy [CAU 02, MAT 96].

### 8.2.4. *Use of a two-phase reference*

The use of reference ($\alpha$, $\beta$) and associated observation methods can still be applied, but electromotive forces can no longer be expressed with the help of simple analytical functions. This reference therefore has no great advantage in this case and can be replaced by a two-phase reference, requiring a transformation that is less

calculation intensive, for example, the reference linked to composites called (ba-ca). The model used is written in the following form:

$$\begin{aligned} V_{ba} &= Rs\cdot(I_b - I_a) + L_{cyc}\cdot\frac{d(I_b - I_a)}{dt} + E_b(\theta) - E_a(\theta) \\ V_{ca} &= Rs\cdot(I_c - I_a) + L_{cyc}\cdot\frac{d(I_c - I_a)}{dt} + E_c(\theta) - E_a(\theta) \end{aligned} \quad [8.4]$$

For the representation in the state space, we assume that the dynamic of the electromotive force is zero. This hypothesis can only be verified if the sampling of frequencies is much higher than the real electromotive force dynamic. If this hypothesis is not verified, representation in reference (ba-ca), or extended Park reference, requires the use of variables that depends on the position and structure of the machine such as $E_{ba}(\theta)$. This requires the tabulation of these variables or their representation by complex analytical functions.

The adaptation of observation methods used for sinusoidal electromotive force machines leads to the finite reconstruction of the position. Even if those generally heavy techniques are not necessary for trapezoid electromotive force machines, they certainly should not be excluded.

## 8.3. Exact reconstruction by redundant observer

Electromechanical equations of the synchronous machine enable the modeling of its dynamic behavior. The use of the Park transformation reduces the complexity of the model and leads to a model in a simplified electric reference of the machine rotating with the rotor. This model, in reference (d, q), for a smooth pole machine ($L_s = L_d = L_q$) is as follows:

$$\begin{bmatrix} Vd \\ Vq \end{bmatrix} = \begin{bmatrix} Rs + pLs & -\omega r \cdot Ls \\ \omega r \cdot Ls & Rs + pLs \end{bmatrix} \begin{bmatrix} Id \\ Iq \end{bmatrix} + Ke\cdot\omega r \begin{bmatrix} 0 \\ 1 \end{bmatrix} \quad [8.5]$$

where $Vd, Vq, Id, Iq$ are the voltage/current dimensions in the stator reference:

$$R_s, L_s, Ke \quad (\sqrt{\frac{3}{2}}Msr.if)$$

and represent stator resistance, stator inductance, and flux produced by the permanent magnets (or the equivalent in the case of an excitation separated, made by

a current *if* through a mutual inductance $M_{sr}$), respectively, which are the parameters of the machine model:

- $\omega r$ is the electric angular speed;
- $p$ the Laplace operator.

For sensorless control (position/speed), we only have the value of estimated position $\tilde{\theta}$.

The two real and estimated angles are linked by the following relation: $\theta_r = \tilde{\theta} + \Delta\theta$. Term $\Delta\theta$ is the estimation position error.

### 8.3.1. *Principle and implementation of analytical redundancy*

According to this diagram (Figure 8.7), electric equations expressed in the estimated rotating reference frame ( $\tilde{d}$ , $\tilde{q}$ ) ( $\tilde{d}$ , $\tilde{q}$ ) are written as:

$$\begin{bmatrix} \tilde{V}d \\ \tilde{V}q \end{bmatrix} = \begin{bmatrix} Rs + pLs & -\omega_{est} \cdot Ls \\ \omega_{est} \cdot Ls & Rs + pLs \end{bmatrix} \begin{bmatrix} \tilde{I}d \\ \tilde{I}q \end{bmatrix} + Ke \cdot \tilde{\omega} \begin{bmatrix} -\sin(\Delta\theta) \\ \cos(\Delta\theta) \end{bmatrix} \quad [8.6]$$

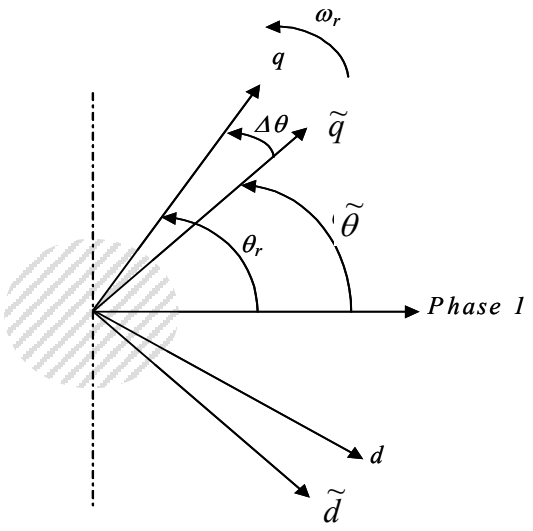


**Figure 8.7.** *Spatiotemporal diagram*

Based on the second line of the above equation, the rotor position and speed can be estimated in the following way:

– by assuming condition $\Delta\theta \cong 0$ (and $\omega_r \cong \tilde{\omega}$) after estimator convergence, the equation can be rearranged by taking cos $(\Delta\theta) = 1$.

The estimation of the estimated speed, according to axis $q$ equations, can be obtained by the following relation:

$$\tilde{\omega}_q = \frac{\tilde{V}q - (Rs + pLs).\tilde{I}q}{Ke + Ls.\tilde{I}d} \quad [8.7]$$

– in transitory conditions $\Delta\theta \neq 0$ and $\omega r \neq \tilde{\omega}$, a correction of the estimation of the previous speed is necessary. The correction is done by using the information redundancy reported by axis $d$ (1st line of equation [8.6]).

In fact, voltage $\tilde{V}d$, under ideal conditions $(\Delta\theta = 0, \tilde{\omega} = \omega r)$ is equal to $V_d$:

$$Vd = (Rs + pLs).\tilde{I}d - Ls.\tilde{\omega}.\tilde{I}q \quad [8.8]$$

Taking sin $(\Delta\theta) = \Delta\theta$, this same voltage can be obtained in case of position estimation error by:

$$\tilde{V}d = (Rs + pLs).\tilde{I}d - Ls.\tilde{\omega}.\tilde{I}q + K_e\tilde{\omega}.\Delta\theta \quad [8.9]$$

We can thus generate a voltage error in axis $d$ that is a function of the position error committed:

$$\Delta\tilde{V}d = Vd - \tilde{V}d \text{ and thus } \Delta\tilde{V}d \cong -Ke.\tilde{\omega}.\Delta\theta \quad [8.10]$$

We can notice that if the error made with $V$ (according to $d$) cancels out $(\Delta Vd = 0)$, then we correctly estimate angle $\theta$ $(\Delta\theta = 0)$, and the speed used is just as correct. We then obtain a complete position, speed, and electromotive force reconstruction of the machine.

Without a speed sensor, canceling this voltage error according to axis $d$ comes down to calculating the electromotive force ($emf_d$):

– on one hand, by using electric parameters $fem_d1 = \tilde{V}d - (Rs + pLs).\tilde{I}d$

– on the other hand, by using rotor speed $fem_d2 = -Ls.\tilde{\omega}.\tilde{I}q$

By using the estimated values, these two electromotive force calculations are including errors but not correlated, that is, the difference between both calculations can only come from an error of projection caused by an error of position injected in the Park transform (Figure 8.8). Or the expression in axis *d* of calculation error $\varepsilon fem_d$ :

$$\varepsilon fem_d = fem_d 1 - fem_d 2 = (\tilde{V}d - Rs.\tilde{I}d - pLs.\tilde{I}d) - (-\tilde{\omega}.Ls.\tilde{I}q) \qquad [8.11]$$

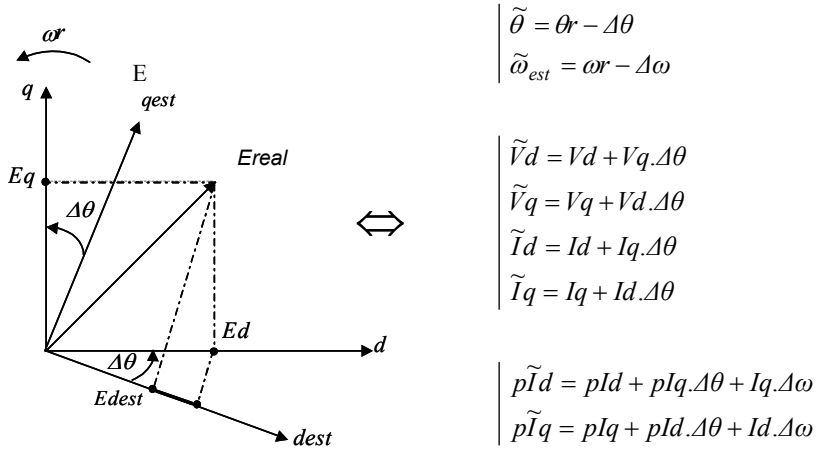


**Figure 8.8.** *General diagram of the MATSUI method principle*

This equation needs speed information. It uses estimated speed according to axis *q*.

We only need to ensure a zero $\varepsilon fem_d$ . By using a PI in this axis, the speed will be corrected and then integrated to give the position. If the system is stable in closed loop, then the PI will ensure that $\varepsilon emf_{\mathrm{d}} = 0$ ($\varepsilon emf_{\mathrm{q}} = 0$), resulting in $\theta = \tilde{\theta}$ (with $\omega = \tilde{\omega}$ , $fem_d = \tilde{f}em_d$ , and $fem_q = \tilde{f}em_q$ ). Or speed correction $\Delta\omega c$ to make:

$$\Delta\omega c = -sign.(\tilde{\omega}_q).(kp + \frac{ki}{p}).\varepsilon fem_d \qquad [8.12]$$

Thus, $\tilde{\omega} = \tilde{\omega}_q + \Delta\omega c$

In different books, it is noted that this method does not work very well in practice. In fact, it involves a derivative on currents ($I_d$, $I_q$) to estimate the position from electric equations in axes ($d$, $q$), which can be penalizing in the case where measurements are noisy. To overcome this problem, a solution can be developed involving a state and disturbance observer avoiding the use of derivatives in currents [SIC 97]. In our case, we directly implemented three filters:

– a filter for voltage ($d$, $q$) eliminating the switching frequency;

– a filter for current derivatives;

– a filter for $\varepsilon emf_d$ ensuring good convergence.

We can see in [8.12] the emergence of the estimated speed signal in axis $q$ to add or subtract information received from the PI. This equation only involves estimated variables, only available in the absence of mechanical sensors. In addition, estimated variables can be expressed according to $\Delta\theta$ and $\Delta\omega$ (presumed small) based on the following relations between the estimated reference system and the real ($d$, $q$) reference system: if $I_d = 0$ (maximum torque control principle) and $\Delta\omega = 0$, we can find equation:

$$\varepsilon fem_d \cong -\omega r.K_e.\Delta\theta \qquad [8.13]$$

The correction of the obtained speed from corrector PI fed by the electromotive force estimation error makes it possible to force the estimate to evolve toward the true value (and vice versa) by using this estimation with errors in the machine control loop.

However, the convergence can be total and stable or partial (therefore, temporarily unstable), that is, either the position or speed is estimated but not both. Three cases appear:

– case no. 1: if the position estimation error $\Delta\theta = 0$, and if estimated speed is correct ($\omega_r = \tilde{\omega}$ or $\Delta\omega = 0$), the redundancy error can only be zero $\varepsilon emf_d = 0$, resulting in a stable estimation of $\theta$ and $\omega$;

– case no. 2: if the error of position cancels $\Delta\theta = 0$, but if speed estimation $\omega_r \neq \tilde{\omega}$ (or $\Delta\omega \neq 0$), then $\varepsilon_{emfd} = +2L_s \cdot I_q$. $\Delta\omega$ will force a speed correction that will immediately increase the error of position, distancing it from the true value, so the estimated speed can catch up to the true speed (case no. 1);

– case no. 3: if the error of position is not zero ($\Delta\theta \neq 0$), but the speed is correctly estimated ($\omega_r = \tilde{\omega}$), then $\varepsilon_{emfd} = \omega_r \cdot K_e$. $\Delta\theta$ will force the speed to move away from an otherwise correct estimation so that the estimated position can reach the true position (case no. 1).

The correction needed is not only a function of its sign alone, but also a function of the rotation sense of the machine. In fact, if an error of position is positive, this may mean a late or early rotation of reference $d$, $q$, since this reference turns with the machine rotor. If the machine turns:

– in the trigonometric direction ($\omega > 0$):

- $\varepsilon_{\text{emfd}} > 0$ ($\Delta\theta < 0$), then $\tilde{\omega}$ should be incremented because we should accelerate to reach true $\theta$;

- $\varepsilon_{\text{emfd}} < 0$ ($\Delta\theta < 0$), then $\tilde{\omega}$ should be decremented because we should slow down to reach true $\theta$;

– in the reverse trigonometric direction ($\omega < 0$):

- $\varepsilon_{\text{emfd}} > 0$ ($\Delta\theta < 0$), then $\tilde{\omega}$ should be incremented because we should accelerate to reach true $\theta$;

- $\varepsilon_{\text{emfd}} < 0$ ($\Delta\theta > 0$), then $\tilde{\omega}$ should be decremented because we should slow down to reach true $\theta$.

In Figure 8.9, the complete representation of the observation method by analytical redundancy is shown.

As shown above, this method leads to focus on problems relating to the physical constraints of the system, such as:

– the adjustment of gains $k_{\text{p}}$, $k_{\text{i}}$, and filters;

– the determination of the initial position;

– sensitivity in relation to the machine's electric parameters.

### 8.3.2. *Adjustment of correction gains*

The observer convergence and stability can not be described by analytical method or Lyapunov approach, there is no way to compute the controller values to insure performance. Below, we will make a few assumptions on $\varepsilon_{\text{emfd}}$ and $\varepsilon_{\text{emfq}}$ expressions, in order to deduce two major relations bringing out rules for choosing factors ($k_{\text{p}}$, $k_i$) according to electric parameters and current $I_{\text{q}}$. This method is mostly based on a vector approach of the behavior of the sensorless self-guided machine and will help us quickly bring out intervals according to criteria of performance.

After the establishment of the representation of the different pieces of information required for the method, we should determine the factors of corrector PI for canceling and linking the error of position to the error of voltage ($\varepsilon_{\text{emfd}}$). In order

to do this, we recall the following parities linked to the block diagram of the observer:

$$\Delta\omega = \omega r - \tilde{\omega} \qquad \tilde{\omega} = \Delta\omega c + \tilde{\omega}_q \text{ and } \Delta\omega c = \left(kp + \frac{ki}{p}\right).\ \varepsilon fem_d \qquad [8.14]$$

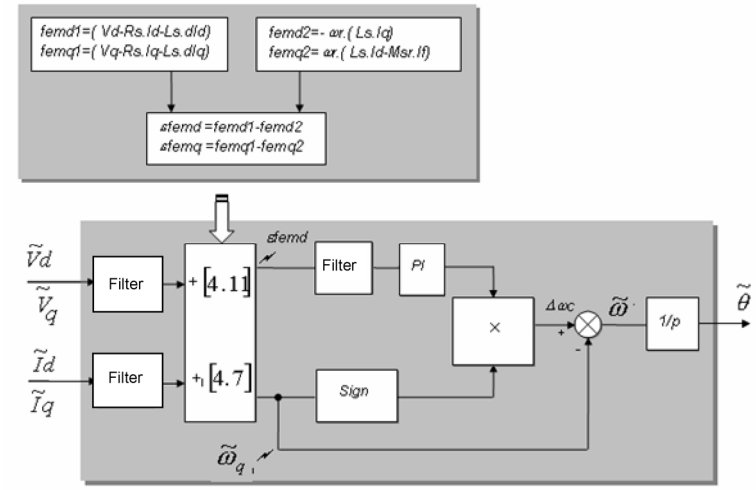


**Figure 8.9.** *Block diagram representation of the method used*

Knowing that $\tilde{I}d \cong 0$, then:

$$\tilde{\omega}_q = \frac{fem_q}{Ke} + \frac{\varepsilon fem_q}{Ke} = \omega r + \frac{\varepsilon fem_q}{Ke} \qquad [8.15]$$

Or the expression of speed error $\Delta\omega$:

$$\begin{aligned} \Delta\omega &= \omega r - kp.\varepsilon fem_d - ki.\int \varepsilon fem_d - \omega r - \frac{\varepsilon fem_q}{Ke} \\ &= -kp.\varepsilon fem_d - ki.\int \varepsilon fem_d - \frac{\varepsilon fem_q}{Ke} \end{aligned} \qquad [8.16]$$

We then obtain an expression of ($k_p$, $k_i$) according to $\varepsilon_{emf}$ ($d$, $q$). Now, we need to find a formulation for the electromotive force error $\varepsilon_{emf}$ ($d$, $q$) in order to easily obtain solvable equations significant of the convergence obtained.

8.3.2.1. *First expression of* $\varepsilon_{\text{emfd}}$, $\varepsilon_{\text{emfq}}$

In the previous section, we calculated the expression of electromotive force error in axis (*d*): $\varepsilon fem_d \cong -Ke.\omega r.\Delta\theta$ with $\Delta\theta \cong 0$ as hypothesis.

In terms of the expression of $\varepsilon_{\text{emfq}}$, we can apply the same methodology, that is, that from the equations of the two matrix lines in *d*, *q*, and from the figure presenting the projections, we can deduce the electromotive force error in axis *q*:

$$\varepsilon fem_q = \tilde{f}em_q 1 - \tilde{f}em_q 2 = (\tilde{V}q - Rs.\tilde{I}q - pLs.\tilde{I}q) + \tilde{\omega}.(Ls.\tilde{I}d - Ke) \quad [8.17]$$

Or, by replacing the expressions of all estimated values by their projection, we get the expression of electromotive force in axis (*q*):

$$\varepsilon fem_q = -2Ls.\omega r.Iq.\Delta\theta + \Delta\omega.Msr.If - Ls.\Delta\omega.Iq.\Delta\theta \quad [8.18]$$

As $I_d \cong 0$ and $\Delta\omega \cong 0$ in the convergence hypothesis, we obtain

$$\varepsilon femq = -2Ls.\omega r.Iq.\Delta\theta$$

Finally, the expressions of $\varepsilon_{\text{emfd}}$ and $\varepsilon_{\text{emfq}}$ are

$$\begin{cases} \varepsilon fem_d = -Ke.\omega r.\Delta\theta \\ \varepsilon fem_q = -2.Ls.\omega r.Iq.\Delta\theta \end{cases} \quad [8.19]$$

If we now use these expressions in the speed equation error in order to cancel it, we have:

$$0 = +kp.Ke.\omega r.\Delta\theta + ki.Ke.\omega r.\int \Delta\theta + \frac{2.Ls.Iq}{Ke}\omega r.\Delta\theta \quad [8.20]$$

If we calculate the derivative in this last equation, then

$$0 = \left[ + \frac{2.Ls.Iq}{Ke}.\Delta\dot{\theta} + Ke.kp.\Delta\dot{\theta} + Ke.ki.\Delta\theta \right] \quad [8.21]$$

and according to $\begin{cases} \dot{U} \\ U \end{cases} = d\frac{\ln U}{dt}$, we have $\Delta\theta = A.e^{rt}$ [8.22]

We can notice that error of position ($\Delta\theta$) will converge over time according to an exponential function in the transitory phase where the hypotheses are respected (the speed already converged).

Thus

$$r = -\frac{Ke^2.ki}{Ke^2.kp + 2.Ls.Iq}$$

By assuming that we can make one of the two terms of the denominator predominant:

$$2.Ls.Iq << Ke^2.kp \text{ , then } r = -\frac{ki}{kp} \qquad [8.23]$$

This disparate relation can then be written as

$$kp.Ke \geq \frac{2.Ls.Iq}{Ke} \ (\cong \omega r)$$

This expression is equivalent to the conditions found by N. Matsui [MAT 96] and B. Mobarakeh [MOB 00]:

$$ki > 0 \text{ and } kp = -\frac{b}{Ke}.sign(\tilde{\omega}_q) \text{ with } b > 0 \qquad [8.24]$$

We can now simulate, in order to validate this parity, with the parameters of a 1.5 kW synchronous machine available on machine builder catalog:

$L_s$ = 0.0533 H; $K_e$ = 0.907 Wb; $I_q$ = 1.25 A

The exponential convergence is only possible after the startup phase in which the speed is established (hypothesis $\Delta\omega \cong 0$). In addition, during this first transitory when speed evolves, the hypotheses are not yet verified and gains quickly contribute to the error of position and make it temporarily lose significant value (Figure 8.10). During the second transitory mode, once the speed is almost established, we notice that if the condition is verified (i.e. that $k_p >> 0$, 26 in this case, gradient $a$ does not respect this case), then $\Delta\theta$ will converge with a not well-defined response time.

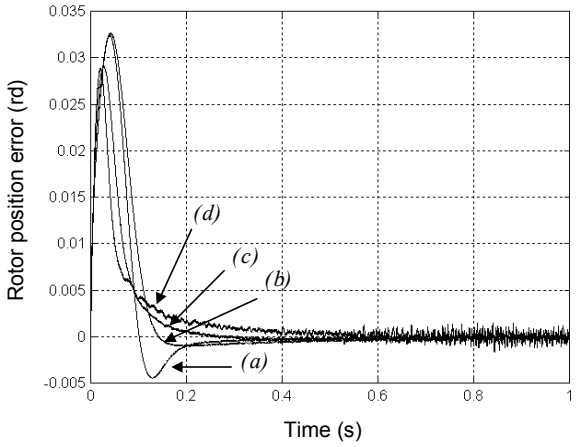


**Figure 8.10.** *Estimation error with different $k_p$, $k_i$ with (a) $k_p = 1$; $k_i = 20$ ($k_i/k_p = 20$); (b) $k_p = 5$; $k_i = 10$ ($k_i/k_p = 2$); (c) $k_p = 2$; $k_i = 10$ ($k_i/k_p = 5$); (d) $k_p = 5$; $k_i = 20$ ($k_i/k_p = 4$)*

The greater $k_i$, the quicker the convergence, but performance depends on the maximum value obtained and uncontrolled in the transitory (very quick gradient for *a-curve* but turns around 0), finally *c* is the best convergence gradient with large factors, but with a $k_i/k_p$ ratio that is not too excessive. In addition, we can see that if $k_p$ is great, the amplitude linked to the first transitory tends to decrease, but noise appears (curve *d*). In terms of gain $k_i$, the greater it is, the more risks of noise and over shoots (curves *d* and *a*).

In conclusion, we have found a first relation, only helping in "limiting" gain $k_p$. Nevertheless, we saw that the value of factor $k_i$ plays a role in response time. Consequently, an additional study is necessary to determine gain $k_i$. We can, however, note the performance of the observer since a simple proportional gain ensures zero error in sinusoidal mode.

8.3.2.2. *Second expression of* $\varepsilon_{emfd}$, $\varepsilon_{emfq}$

We recall the expression of $\varepsilon_{emfd}$: $\varepsilon fem_d = -Ke.\omega r.\sin \Delta\theta$ . By projection in axis ($q$), we have $\varepsilon fem_q = +Ke.\omega r - Ke.\omega r.\cos \Delta\theta$ .

From here, we use equation [8.16], and by using these values, we have

$$\Delta\omega = +kp.Ke.\omega r.\sin \Delta\theta + ki.Ke.\omega r.\int \sin \Delta\theta dt - \omega r + \omega r.\cos \Delta\theta \qquad [8.25]$$

hence a condition for canceling the speed error, and if we assume that speed variations are small in the integration time interval, we get:

$$0 = \omega r.(kp.Ke.\sin \Delta\theta - ki.Ke.\cos \Delta\theta + \cos \Delta\theta - 1) \quad [8.26]$$

And now, if we say:

$$\begin{cases} \alpha = kp.Ke \\ \beta = (1 - Ke.ki) \end{cases} \text{ we have } \alpha.\sin \Delta\theta + \beta.\cos \Delta\theta = 1 \quad [8.27]$$

To use this last equation, we will limit the allowable position error:

$$-\frac{\pi}{4} < \Delta\theta < \frac{\pi}{4} \text{ or } \frac{1}{\sqrt{2}} < \cos \Delta\theta < 1 \text{ and } \frac{1}{\sqrt{2}} < \frac{1 - \alpha.\sin \Delta\theta}{\beta} < 1 \quad [8.28]$$

In fact, to have a rotation in the desired direction (given by the sign of reference current), it is necessary to apply a current that is not "opposed" to the closest magnet, which would result in turning the machine in the opposite direction if it can follow the field created (possibility of stalling).

Because of this, the prior initialization value of the estimation program for the position of the rotor should be known by detection methods of the initial position at idle, or by pre-positioning of the rotor. For a two poles pair machine in our case, $\pm\pi/4$ is the angular limit of the operation zone not requiring the involvement of the step called "initial positioning".

For the parameters of the machine chosen: $ki >> 0{,}35 + kp.\sin 2\Delta\theta$

From this expression, we can notice once more that if the parameters of equations are known, and if the initial position error is zero, then gain $k_i$ can be low, without hindering the convergence. On the other hand, if $\Delta\theta$ is involved (0.8 rad in initial value in the following simulations), then $k_i$ is involved. We will now simulate this last equation.

In figure 8.11, we notice that if the choice of coefficient $k_i$ verifies the equation (curves (*b*) and (c), at the limit for (*d* )), the error of position converges toward zero. Nevertheless, if gain $k_i$ is too significant, $\Delta\theta$ tends to be disturbed by current noise (current providing torque and thus a certain motor speed). In fact, the amplitude of current $I_q$ sets the machine's rotation speed for a given load.

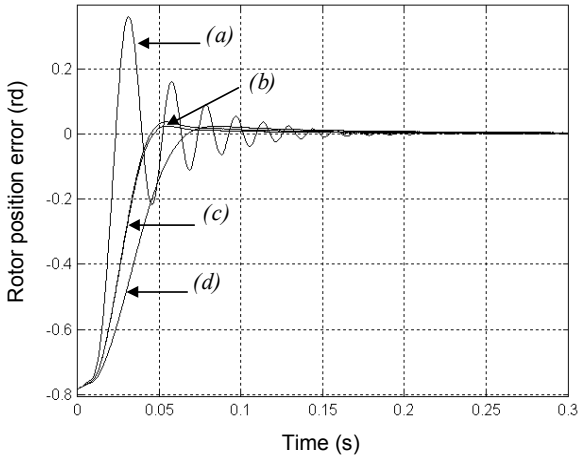


(a)

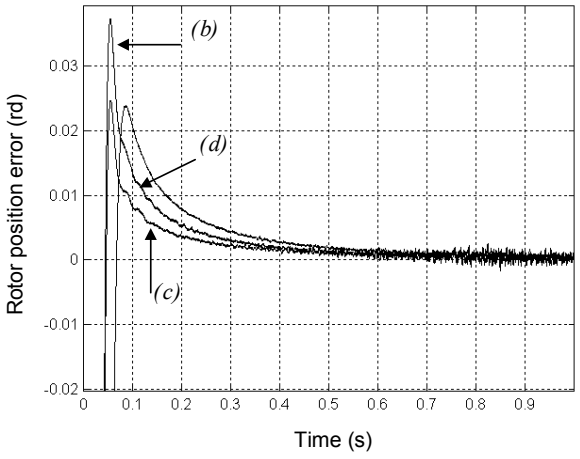


(b)

**Figure 8.11.** *Determination of operation zones with (a)* $k_p = 5$*;* $k_i = 0.2$ *(*$k_i/k_p = 0.04$*); (b)* $k_p = 0.3$*;* $k_i = 5$ *(*$k_i/k_p = 17$*); (c)* $k_p = 0.2$*:* $k_i = 3$ *(*$k_i/k_p = 15$*); (d)* $k_p = 0.2$*;* $k_i = 2$ *(*$k_i/k_p = 20$*)*

In conclusion, if we combine the expressions of $k_p$ and $k_i$ verified in simulation, we can determine in Figure 8.12 an operation zone in relation to "acceptable" values of $k_p$ and $k_i$, for a correct system behavior.

Operation should be stable and convergent without too much noise in sinusoidal mode estimations, limiting that gains not be too high.

In addition, we should be able to control transitory behavior, and notably, that linked to sometimes significant errors of position. This mandates that rating gains ($I_q$) should be adapted and should take adequate values in relation to the $k_p/k_i$ ratio.

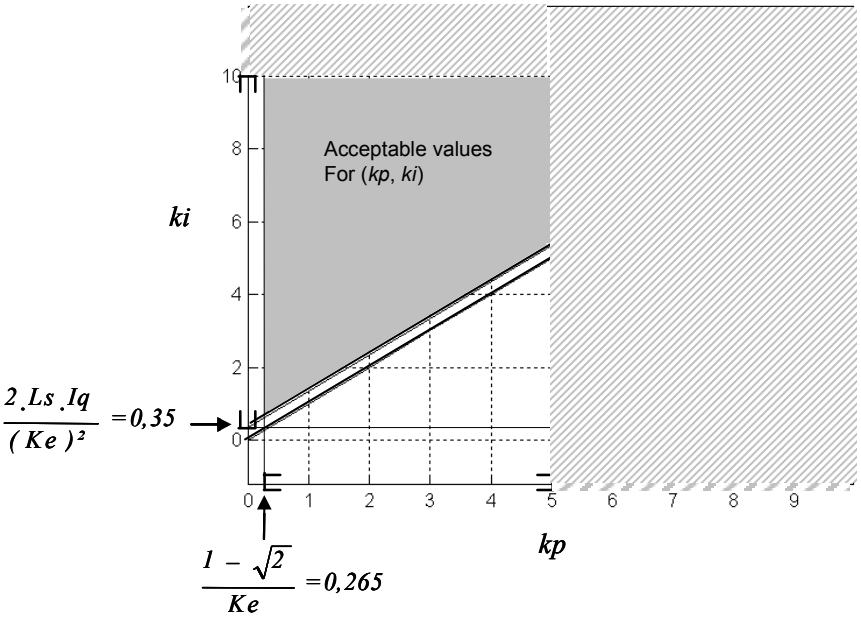


**Figure 8.12.** *Choice of gains ($k_p$, $k_i$). The lined zone corresponds to the zone of large gains and very noisy signals*

8.3.2.3. *Adjustment of the analytical redundancy observer with filters*

Because of the relation between electromotive force error and the error of position estimation, we know intuitively that an increase in gains will lead to a quicker or stronger correction of estimation errors. However, the filters should have a cut-off frequency that is high enough to let information go through while eliminating noise, which would cause a modification of the estimation linked to noise, and not to an actual error.

First of all, the speed estimate is very noisy see Figure 8.13. In fact, the predominant term in the estimated speed expression is voltage $V_q$. We then find noises from the division of the switched-supply voltage of the machine in the speed observed.

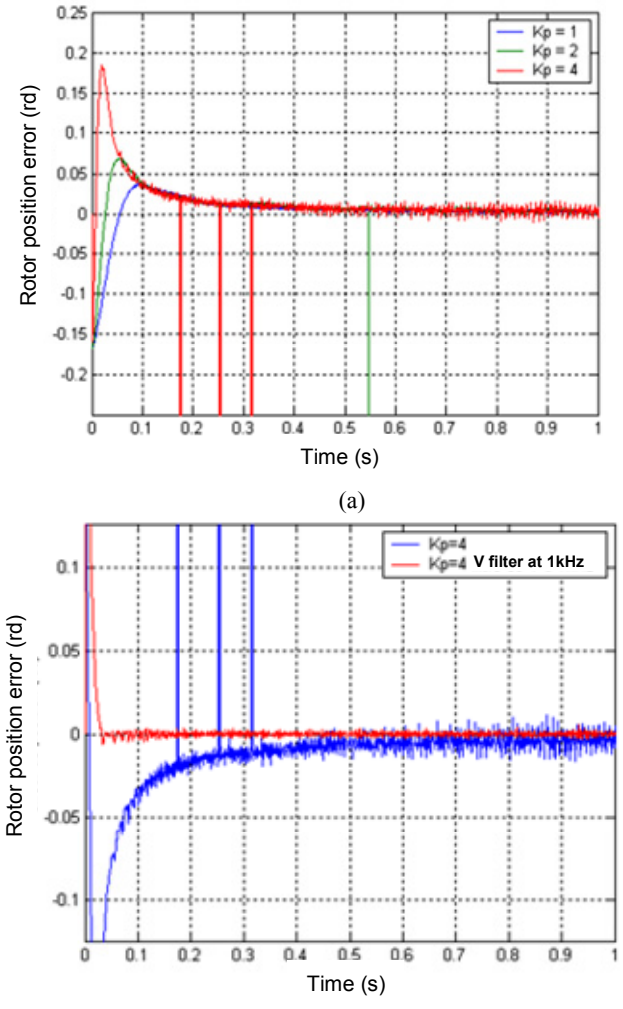


**Figure 8.13.** *Position error for different $k_p$ gains and with filtering*

However, this high noise does not prevent the convergence of the position error. On the other hand, this mandates a correction of the effect of dead times in order to calculate *d*, *q* voltage from control orders. The integration between speed and position estimates makes it possible to efficiently smooth the position calculated. The convergence of the position estimation is rapidly effective with an accuracy of about one mechanical degree.

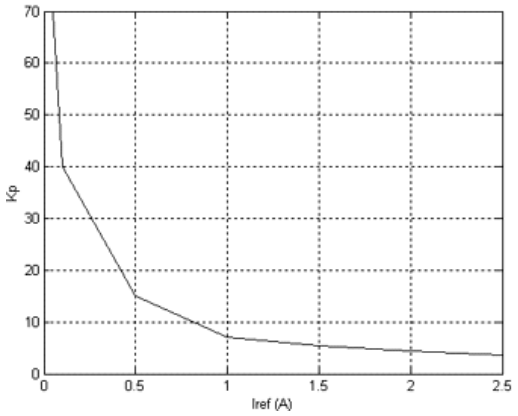


**Figure 8.14.** *Maximum $k_p$ according to $I_{ref}$ rms value of the line current*

The dynamic imposed by the regulation of currents (amplitude $I_{ref}$ and desired response time in the current), placed before the observer, causes a clear increase in the position estimate, whereas the machine has not started turning yet. But the effects of the correction are quickly felt and bring the estimate back to the real value. Other tests also show that this peak of the position error increases when the reference current increases (hyperbolic relation between gain $k_p$ and the current to impose $I_q$, Figure 8.14).

In order to accelerate the convergence of the position estimate, we increased $k_p$, which involves a quicker consideration of position errors and a stronger correction.

The lower the cut-off frequency of the filter, the lower the limit speed. In fact, the electromotive force error and corrective action are linked to the rotation speed and position error. As the speed increases, the correction gets faster and noise levels become more significant. The voltage filter then cuts off information necessary to the correction. The filter creates a delay that is significant enough for errors to greatly increase, and when the corrective action detects them, it is even stronger and the phenomenon can happen again.

On the other hand, for lower gains $k_p$, the filter plays a role and decreases noises on the estimate regardless of the rotation speed. In addition, cutting noises linked to the switch frequency clearly improves convergence time (very small overshoot). Voltage filtering also reduces noises in speed estimation, which is useful in implementing a loop that controls the speed of the synchronous machine.

8.3.2.4. *Adjustment of gains and filter in relation to the reference current*

As we have seen before, current reference $I_{ref}$ has an influence on the position error at startup and generates significant noises if proportional gain $k_p$ is too high. In addition, $I_{ref}$, current amplitude $I_q$, is therefore directly linked to the electromagnetic torque of the machine. A rotation speed in sinusoidal mode is also deducted from the mechanical equation of the machine for a given load.

The dependence between $k_p$ and the rotation speed image of $I_q$ appears in relation:

$$kp \geq \frac{2.Ls.Iq}{(Ke)^2} \geq \frac{\omega r}{Ke}$$

but with condition:

$$kp \leq \frac{c_1}{Iq}$$

thus reducing the influence of gain $k_i$.

For a given choice of voltage filter, there is a law linking maximum gain $k_p$ and the rms value of the reference current with the help of coefficient $c_1$, which we cannot calculate in an analytical way. We determine, by simulation, maximum gains $k_p$ ensuring convergence for a filter placed at 10 kHz.

We prefer to use gains close to this limit for quick convergence. We should also avoid gains that are too small for low currents because convergence is then very slow. If we place the voltage filter at a lower frequency, the gain limitation would be greater.

Because of the efficiency with which the estimated position converges with its real value when gain $k_p$ is well calibrated with the chosen voltage filter, gain $k_i$ usefulness is minor (Figure 8.15). In fact, in order for gain $k_i$ to have a significant effect, we should set it up at a very high value. In addition, it does not improve convergence time and even creates additional oscillations caused by resulting noises. We should therefore choose a proportional regulator.

Knowledge of this function linking proportional gain to the reference current enables the use of an adaptive gain for a constant optimal estimate. However, these gains are also linked to the machine's rotation speed. Strong reference current variation with strong gain and high speed can lead to a disruption such that the observer cannot ensure continuity of convergence. In order to see the effect and importance of gains and the different filter cut-off frequencies, a study from

experimental designs approach confirmed the importance of gain $k_p$, and the influence the reference current (motor rotation) has on observer performances [CAU 06].

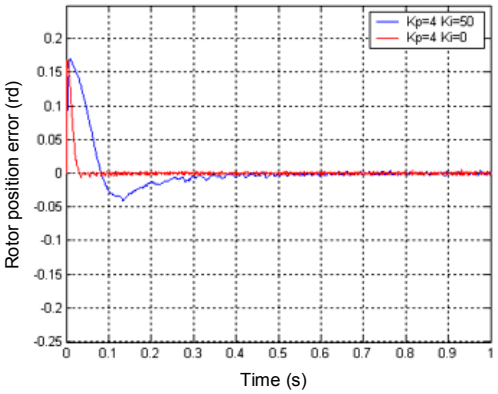


**Figure 8.15.** *Addition of an integral gain disrupting performance*

We should place a saturation or a filter on the basis information from the digital derivation of currents. In fact, a derivation of the sampling period on noisy measurements provides erroneous values that disturb the convergence of the algorithm. By calculating the maximum derivative of possible currents (a function of the available bus voltage and value of the motor winding self), a limitation in magnitude takes away the absurd calculated values and lets necessary information go through. A first-order low-pass filter, placed at the switch frequency, also ensures this function without introducing too much phase shifting if the cut-off frequency is high enough.

### 8.3.3. *Sensitivity and robustness*

System performances are generally sensitive to the variations of parameters and precision of measurements. The structure of the position observer with analytical redundancy requires precise knowledge of resistance $R_s$, and inductance $L_s$ and $K_e$.

From the vector representation (Figure 8.16), we notice that not only an initial position error can cause incorrect rotation, but a generally large error on an electric parameter ($R_s$ in this case) can also contribute to incorrect behavior. In fact, a significant gap in this factor distorts speed, and estimated position is very far from the real position. The justification of correct operation sectors has already been given in the comment in equation [8.28].

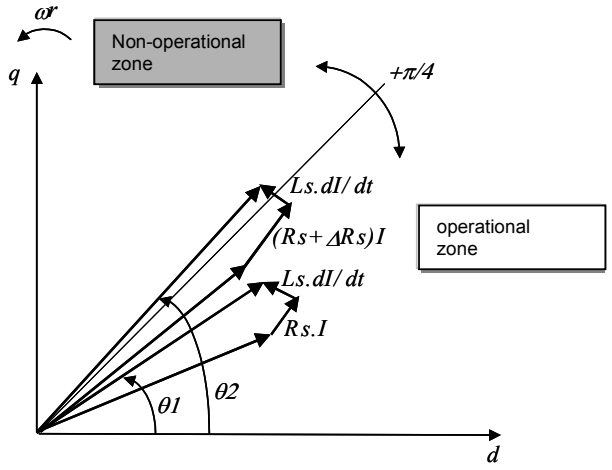


**Figure 8.16.** *Vector representation of a two pair pole machine*

In order to correct a hypothetical error of position, caused by an excessive variation in an electric parameter, we developed a "calibration" method to find out and correct the variation of the parameter in the algorithm in order to cancel the error of position.

The consequence of the parameter error in the final position value is easily determined with the help of the vector diagram. If ratio $(\Delta R \cdot I_q)/V_d$ is small, we obtain the final expression:

$$\Delta\theta_R = \text{atan}.\frac{Vd.Iq.\Delta R}{(Vd)^2 + (Rs.Iq - \omega r.Ke)^2} \qquad [8.29]$$

In what follows, we generalize the precise methodology of evaluation of the error made on the position and electric parameters followed by the study of robustness in relation to $R_s$. If, for example, we accept a significant variation of $R_s$, the electric equations in reference frame (d, q) are:

$$\begin{bmatrix} \tilde{V}d \\ \tilde{V}q \end{bmatrix} = \begin{bmatrix} (Rs + \Delta Rs) + pLs & -\tilde{\omega} \cdot Ls \\ \tilde{\omega}_t \cdot Ls & (Rs + \Delta Rs) + pLs \end{bmatrix} \begin{bmatrix} \tilde{I}d \\ \tilde{I}q \end{bmatrix} + Ke \cdot \tilde{\omega} \begin{bmatrix} 0 \\ 1 \end{bmatrix} \qquad [8.30]$$

The equation based on axis ($d$) gives the electromotive force error (proportional to $\Delta\theta$), and the one based on axis $q$ is used to extract a speed estimation using estimated voltage and currents (the Park transform involves the estimated position) ([8.7] and [8.13]).

Since $\Delta\theta$ ($\Delta\theta = \tilde{\theta} - \theta_{real}$) is not known because $\theta_{real}$ is not measured (no position sensor), information on $\tilde{\omega}_q$ alone remains in order to find a relation expressing the variation of the parameter.

According to the equation including a variation of $R_s$, an incorrect estimation of permanent speed (with $(p\tilde{I}q = \tilde{I}d = 0)$ is expressed as follows:

$$\tilde{\omega} = \frac{\tilde{V}q - (Rs + \Delta Rs).\tilde{I}q}{Ke} \text{ and by observer } \tilde{\omega} = \tilde{\omega}_q + \Delta\omega c \qquad [8.31]$$

According to these equations, the expression of $\Delta\omega c$ based on variation $\Delta R_s$ is:

$$\Delta\omega c = -\frac{\Delta Rs}{Ke}.Iq \qquad [8.32]$$

This last equation gives the exact error on $R_s$ using the corrector output. The correction of this variation in the algorithm now makes it possible to cancel the error of position. The position gap, caused by a variation in $R_s$, can also be quantified by a written formula with the help of electric equations. This formula, based on an error of position, in practice, cannot help with the correction because there is no measure of position.

Finally, the calibration method occurs in the following way: in the first step, we estimate speed and position with incorrect parameters. When the speed has reached its nominal mode, we know value $\Delta\omega c$ and correct parameter $R_s$. In order to do this, we add a speed test at two different moments, and when this speed is identical, we update parameters $R_s$ ($R_s = R_s + \Delta R_s$) to obtain a representative value of the machine. In this way, after this calibration step, the algorithm calculates with the real parameter value.

Stator resistance mainly evolves according to temperature variations triggered by the evolution of current and rotation frequency of the machine.

We deduce the expression of $\Delta R_s$ according to $\Delta\omega c$:

$$\Delta Rs = \frac{\Delta\omega c.Ke}{Iq} \qquad [8.33]$$

As $\Delta\omega c$ is the correction used for velocity, we use the PI output of the Matsui structure to calculate $\Delta R_s$. After a calibration phase, we correct $\tilde{R}s = Rs - \Delta Rs$. In Figure 8.17, the correction of $R_s$ is shown during complete simulation of speed driving of a synchronous machine without mechanical sensor and the convergence of estimated velocity in two phases. After the initial positioning phase of 4 s, the synchronous machine reaches its sinusoidal mode at $t$ = 6 s. During the transitory mode, stator resistance equals $R_s + \Delta R_s$. When velocity reaches its nominal mode, we digitally calculate the value of $\Delta R_s$ from electric variables at moment 6 s + $\Delta t$. During period $\Delta t$ set at 0.25 s, we calculate the mean value of electric variables making it possible to calculate $\Delta R_s$. Then, we re-inject the new stator resistance value in the algorithm. Since $R_s$ is correct, the estimations are also correct (Figure 8.17 – speed and resistance, Figure 8.18 emf).

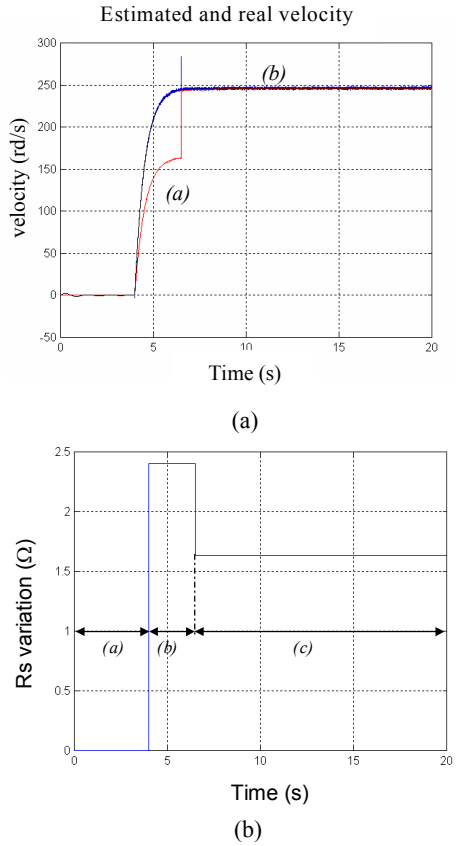


**Figure 8.17.** *Visualization of real velocity and $R_s$ correction with (a) ((a) estimated velocity; (b) real velocity); (b) ((a) shifting phase; (b) calibration phase; (c) Rs correction)*

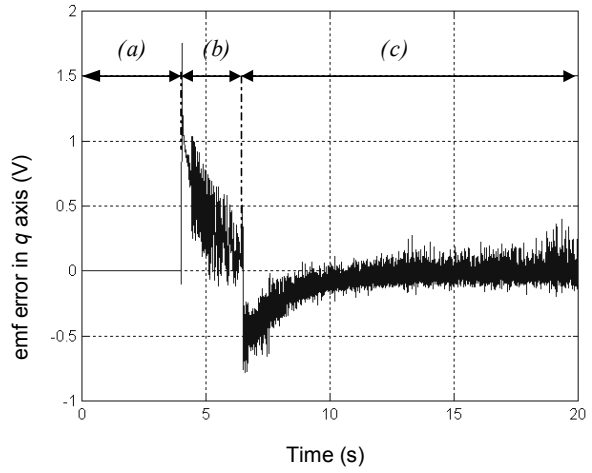


**Figure 8.18.** *Variation of electromotive force with (a) shifting phase; (b) calibration phase (convergence to an interrupted non-zero error); (c) correct operation (initial disruption because of change in $R_s$ value in equations, then convergence to a zero estimation error)*

### 8.3.4. *Experimental results*

The algorithm was implemented for obtaining the first experimental tests given below.

The synchronous machine used is an industrial grade motor[1] with the following characteristics:

| | |
|---|---|
| Nn = 3,000 rpm | In = 8.5 A |
| Fn = 150 Hz | Rs = 0.55 Ω |
| emf = 80 V/1,000 rpm | Lsd = Lsq = 8.5 mH |

In Figure 8.19a, the rotor positioning is obtained by injecting a current of 2 A in axis ($d$), followed by a startup of 0 to 300 rpm. This test makes it possible to visualize the correct observer behavior.

In Figure 8.19b, a startup of 0 to 1,000 rpm is shown. The estimated velocity follows the real velocity on the basis of the imposed cycle, even though the PI corrector of the observer was not adjusted more precisely. There is only a proportional gain, and because of initial positioning step, the $k_i$ effect is minimal.

1 With thanks to LEROY-SOMMER.

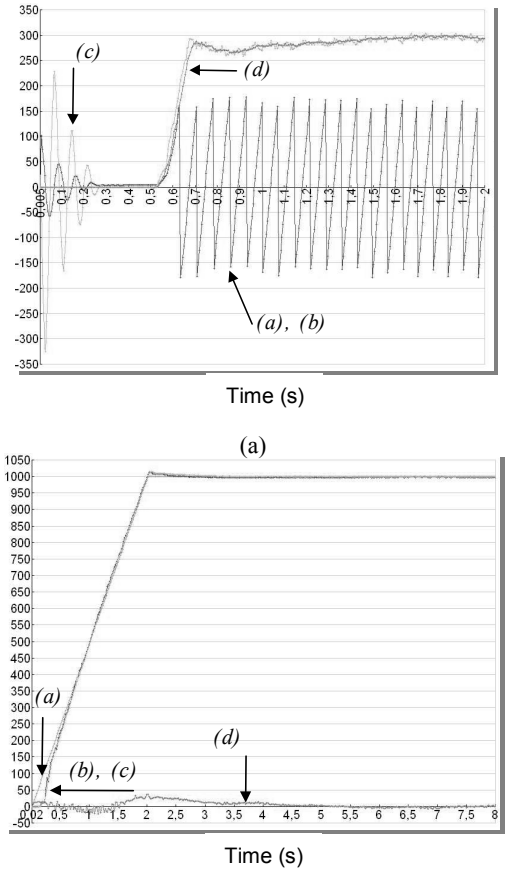


**Figure 8.19.** *Experimental tests (a) validation of the initial step ((a) real position, (b) estimated position, (c) real velocity, (d) estimated velocity); (b) response to a reference in speed* $r_{amp}$ + 1,000 *rpm ((a) reference velocity, (b) real velocity, (c) estimated velocity, (d)* $\varepsilon_{emfd}$ *)*

Experimentally, the voltage is rebuilt using the DC-bus voltage and IGBT orders with compensation of dead times to delete as many sensors as possible. For low-duty-cycle relations, it is necessary to compensate the effect of converter dead times in order to feed the observer equations with voltage that is the closest to reality. This makes it possible to have information on additional sensorless voltage by avoiding filtering problems.

Current regulation achieved continuously in the rotating reference frame ($d$, $q$), controls current components $d$ and $q$ and thus torque. PI-type current regulators are easily defined from parameters $R$, $L$ of the machine. This is implemented in an industrial variable speed drive ready to be commercialized.

## 8.4. Exact reconstruction by Kalman filter

### 8.4.1. *Overview*

The Kalman filter is a reference method of the state reconstruction and one of the great discoveries in the field of systems control and estimation. It plays a vital role in automatic and signal processing world.

Using the state representation of linear systems, the Kalman observer provides, in recursive form and all the time, the optimal estimate and variation of the estimation error (Figure 8.20). Its formulation is particularly adapted to discrete systems and to the implementation by using computer for real-time processing.

The Kalman filter is a stochastic observer for the reconstruction of state $X_k$ of the system from:

– input signals represented by input vector $U_k$;

– measures represented by vector of measure $Y_k$;

– its sampled model defined by matrices $A_k$, $B_k$, and $C_k$;

– noises: state noise $W_k$ representing the non-deterministic part such as modeling errors or external disruptions and measure noise $V_k$ including sensor imperfections.

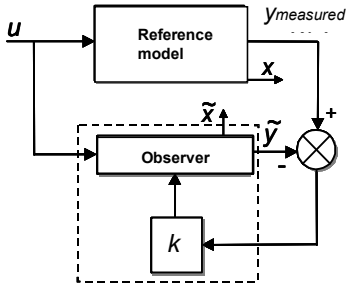


**Figure 8.20.** *Principle of the state observer*

The noisy linear system is described by the following state equations:

$$\begin{cases} X_{k+1} = A_k.X_k + B_k.U_k + W_k \\ Y_k = C_k.X_k + V_k \end{cases} \quad [8.34]$$

However, we suppose that disturbance vectors $W_k$ and $V_k$ are non-correlated Gaussian white noises characterized by:

– zero mean values: $E(W_k) = 0$ and $E(V_k) = 0$;
– the independence of measure and state noises: $E\left(W_k V_j^T\right) = 0$;
– covariance matrices such as:

$$E\left(W_k W_j^T\right) = \begin{cases} Q_k & j = k \\ 0 & j \neq k \end{cases} \text{ and } E\left(V_k V_j^T\right) = \begin{cases} R_k & j = k \\ 0 & j \neq k \end{cases}$$

Even though the Kalman filter is optimal, leading to a minimum error variance, the determination of matrices $Q_k$ and $R_k$ represents the main problem when using the Kalman filter. In fact, noise characteristics are generally not well known.

We will note $\hat{X}_{(k+1/k)}$ the prior estimation of vector $\hat{X}_{(k+1)}$ from information that we have at moment $k$. The implementation of the discrete Kalman filter is split into three steps.

An initialization phase, a prediction phase during which the state at moment $(k+1)T_e$ is estimated according to the state and measures taken at moment $kT_e$ followed by an actual correction phase. The recurring equations used for the prediction are those from the deterministic model [8.34].

$\hat{X}_{(k+1/k)}$ is the prior estimation of the dimension $n$ state, since at calculation moment $(kT_e)$, measurement $y_{(k+1)}$ is not yet known. Vector $\hat{X}_{(k/k)}$ represents the estimation of $X$ at moment $(kT_e)$ following the consideration of measures at the same moment. It is therefore a later estimation of the state.

We also define the covariance matrices of observation errors, associated with vectors $\hat{X}_{(k+1/k)}$ and $\hat{X}_{(k/k)}$ by:

$$\begin{aligned} P_{(k/k-1)} &= E\left\{(\hat{X}_{(k/k-1)} - X_{(k)}).(\hat{X}_{(k/k-1)} - X_{(k)})^T\right\} \\ P_{(k/k)} &= E\left\{(\hat{X}_{(k/k)} - X_{(k)}).(\hat{X}_{(k/k)} - X_{(k)})^T\right\} \end{aligned} \quad [8.35]$$

where $P_{(k/k-1)}$ and $P_{(k)}$ are defined as positive. They give an indication on the precision of estimations. The projection of matrix $P_{(k+1/k)}$ is:

$$P(k+1/k) = A(k) \cdot P(k) \cdot A^T(k) + Q(k)$$

These recursive equations are done at each sampling period. The covariance matrices can lose their symmetry and lead to filter instability. This problem can be avoided if we only use their upper or lower triangular part in the calculations.

The correction phase consists of updating the estimation of state $\hat{X}_{(k/k)}$ from the measure at that moment and prior estimation $\hat{X}_{(k/k-1)}$:

$$\hat{X}_{(k/k)} = \hat{X}_{(k/k-1)} + K_{(k)} . (y_{(k)} - C_{(k)} . \hat{X}_{(k/k-1)}) \quad [8.36]$$

Optimal gain $K$ ($k$) in the sense of prior variance minimization of the estimation error is calculated as follows.

The covariance matrix should also be updated and we therefore find:

$$P_{(k/k)} = (I_{nxn} - K_{(k)} \cdot C_{(k)}) \cdot P_{(k/k-1)} \quad [8.37]$$

where $P_{(k/k)}$ is the covariance matrix *a posteriori* and:

$$K_{(k)} = P_{(k/k-1)} \cdot C_{(k)}^T \cdot (C_{(k)} \cdot P_{(k/k-1)} \cdot C_{(k)}^T + R_{(k)})^{-1} \quad [8.38]$$

In traditional deterministic observers, inverse feedback gains are determined in order to impose the desired convergence dynamic (Luenberger). In the Kalman filter, matrix $K$ is determined to minimize the average of the quadratic estimation error. The correction phase consists in updating prior estimations $\hat{X}_{(k/k-1)}$ and the corresponding estimation error covariance $P_{(k/k-1)}$ from the new measurement at that moment. This correction is based on the calculation of $K_{(k)}$ that should be done first. From updated state variables and covariance matrix at moment $k$, the prediction phase consists of projecting them at moment $k + 1$ using the system knowledge model.

The Kalman filter algorithm is split into three phases:

– an *initialization phase*, from the estimated state $\hat{X}_{0|0} = X_0$, and the covariance matrix of observation errors $\hat{P}_{0|0} = P_0$;

– a *prediction phase*, where we make a prior estimation of:

- state $\hat{X}_{k+1|k}$ at moment $(k + 1)\ T_e$, without knowledge of measures $Y_{k+1}$, and from estimation $\hat{X}_{k|k}$ at moment $k \cdot T_e$:

$$\hat{X}_{k+1|k} = A_k.\hat{X}_{k|k} + B_k.U_k \qquad [8.39]$$

- the covariance error matrix:

$$P_{k+1|k} = A_k.P_{k|k}.{A_k}^T + Q_k \qquad [8.40]$$

– a *correction phase*, where an update is executed: the estimation of state $\hat{X}_{k+1|k+1}$ taking into consideration prior state $\hat{X}_{k+1|k}$, measures $Y_{k+1}$, and Kalman gain $K_{k+1}$ weighing the error between measures and their estimations *a priori*:

$$\hat{X}_{k+1|k+1} = \hat{X}_{k+1|k} + K_{k+1}.(Y_{k+1} - \hat{Y}_{k+1|k}) \qquad [8.41]$$

with $\hat{Y}_{k+1|k} = C_k.\hat{X}_{k+1|k}$ we obtain:

$$\hat{X}_{k+1|k+1} = \hat{X}_{k+1|k} + K_{k+1}.(Y_{k+1} - C_{k+1}.\hat{X}_{k+1|k}) \qquad [8.42]$$

the covariance matrix:

$$P_{k+1|k+1} = (I - K_{k+1}.C_{k+1}).P_{k+1|k} \qquad [8.43]$$

and the Kalman gain:

$$K_{k+1} = P_{k+1|k}.{C_{k+1}}^T.(C_{k+1}.P_{k+1|k}.{C_{k+1}}^T + R_{k+1})^{-1} \qquad [8.44]$$

We then obtain the standard Kalman algorithm where the correction and prediction phases are detailed in Figure 8.21.

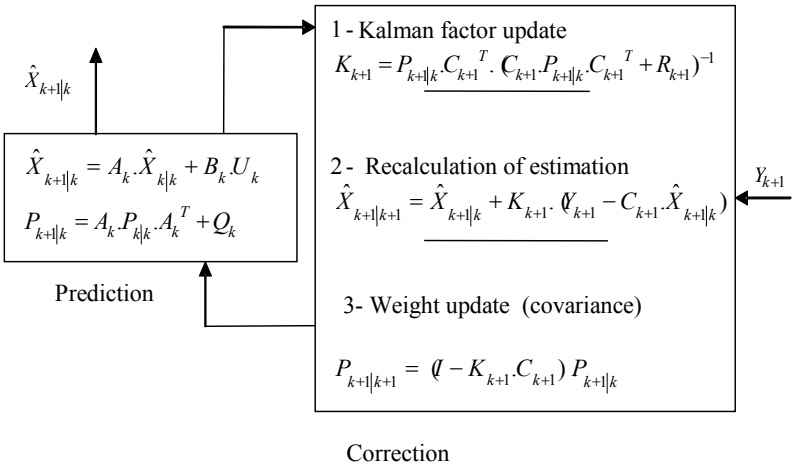


**Figure 8.21.** *Discrete Kalman algorithm*

### 8.4.2. *Using the Kalman filter for the synchronous machine without mechanical sensor*

The application of the standard Kalman algorithm is restricted because the linear representation is only rarely verified for physical systems. In this case, we will use another formulation of the Kalman filter, consisting of first executing a limited serial of Taylor order 1 development to be able to linearize the system, and apply the standard Kalman filter.

The noisy linear system is described by the following state equations:

$$\begin{cases} X_{k+1} = f(k, X_k, U_k, W_k) \\ Y_k = h(k, X_k, V_k) \end{cases}$$

In the necessary derivability hypotheses, we obtain with the limited order 1 development approximately $X_k^{\,e}$ for state equation and $X_k^{\,m}$ for the measure equation:

$$\begin{cases} X_{k+1} = f(k, X_k^{\,e}, U_k, 0) + \dfrac{\partial}{\partial X} f\Big|_{X_k^{\,e}}.(X_k - X_k^{\,e}) + \dfrac{\partial}{\partial W} f\Big|_{0}.W_k \\ Y_k = h(k, X_k^{\,m}, V_k) + \dfrac{\partial}{\partial X} h\Big|_{X_k^{\,m}}.(X_k - X_k^{\,m}) + \dfrac{\partial}{\partial V} h\Big|_{0}.V_k \end{cases} \quad [8.45]$$

or:

$$\begin{cases} X_{k+1} = F_k.X_k + U_k{}^e + D_k.W_k \\ Y_k = H_k.X_k + U_k{}^m + E_k.V_k \end{cases} \quad [8.46]$$

where

$$\begin{cases} F_k = \dfrac{\partial}{\partial X} f\Big|_{X_k{}^e}, \quad D_k = \dfrac{\partial}{\partial W} f\Big|_0 \quad H_k = \dfrac{\partial}{\partial X} h\Big|_{X_k{}^m}, \quad E_k = \dfrac{\partial}{\partial V} h\Big|_0 \\ U_k{}^e = f(k, X_k{}^e, U_k, 0) - F_k.X_k{}^e, \quad U_k{}^m = f(k, X_k{}^m, V_k) - H_k.X_k{}^m \end{cases}$$

We then obtain the new equations making up the Kalman algorithm: for the prediction phase:

$$\hat{X}_{k+1|k} = F_k.\hat{X}_{k|k} + U_k{}^e$$

linearized around $X_k{}^e = \hat{X}_{k|k}$, or:

$$\hat{X}_{k+1|k} = f(k, \hat{X}_{k|k}, U_k, 0) \quad [8.47]$$

$$P_{k+1|k} = F_k.P_{k|k}.F_k{}^T + D_k.Q_k.D_k{}^T \quad [8.48]$$

For the correction phase:

$$\hat{Y}_{k+1|k} = H_{k+1}.\hat{X}_{k+1|k} + U_{k+1}{}^m$$

linearized around: $\hat{X}_k^m = .\hat{X}_{k+1|k}$, or, $\hat{Y}_{k+1|k} = h\left(k+1, \hat{X}_{k+1|k}, 0\right)$ hence:

$$\hat{X}_{k+1|k+1} = \hat{X}_{k+1|k} + K_{k+1}.\left(Y_{k+1} - h(k+1, \hat{X}_{k+1|k}, 0)\right) \quad [8.49]$$

with:

$$K_{k+1} = P_{k+1|k}.H_{k+1}{}^T.(H_{k+1}.P_{k+1|k}.H_{k+1}{}^T + E_{k+1}.R_{k+1}.E_{k+1}{}^T)^{-1} \quad [8.50]$$

$$P_{k+1|k+1} = (I - K_{k+1}.H_{k+1}).P_{k+1|k} \quad [8.51]$$

### 8.4.3. *Application for the synchronous machine*

By considering the smooth pole synchronous machine model developed previously in rotating reference frame *d*, *q* (section 8.3) with the Park transform, we have:

$$\begin{cases} \dfrac{dId}{dt} = \dfrac{Vd}{Ls} - \dfrac{Rs}{Ls} Id + \omega.Iq \\ \dfrac{dIq}{dt} = \dfrac{Vq}{Ls} - \dfrac{Rs}{Ls} Iq - \omega.Id - \dfrac{Ke}{Ls}\omega \end{cases} \quad [8.52]$$

We then add the mechanical equation of the machine, linking the torque to the rotation speed:

$$J.\frac{d\Omega}{dt} + f.\Omega = Cem - Cr \quad [8.53]$$

with: $Cem = Np.Ke.Iq$ and $\omega = Np.\Omega$ where $\Omega$ is the mechanical speed, $\omega$ the electric angular frequency, $C_{em}$ the electromagnetic torque, $C_r$ the resistive torque, $J$ the rotor inertia (or all turning parts, load included), $f$ the friction factor, and $N_p$ the number of poles.

Or,

$$\frac{d\omega}{dt} = \frac{Np^2.Ke}{J}.Iq - \frac{f}{J}.\omega - \frac{Np}{J}.Cr \quad [8.54]$$

We then have an order 3 state representation with $I_d$, $I_q$, $\omega$ as state variables. The reconstruction of the position can then be done in two ways:

By directly applying the Kalman filter to this state representation, then integrating the estimated speed from a known initial position.

Or by increasing the order of the representation by adding the position as state variable, then applying Kalman to this new representation, which is 4th order this time.

Since the previous order 3 state representation showed weaknesses in the position estimation in previous studies [PEY 03], we will only focus on the second

alternative. We then obtain the following order 4 state representation (by writing $\tau = L_S/R_S$ as the electric time constant):

$$\begin{cases} \begin{bmatrix} \dot{Id} \\ \dot{Iq} \\ \dot{\omega} \\ \dot{\theta} \end{bmatrix} = \begin{bmatrix} -\frac{1}{\tau} & \omega & 0 & 0 \\ -\omega & -\frac{1}{\tau} & -\frac{Ke}{Ls} & 0 \\ 0 & \frac{Np^2.Ke}{J} & -\frac{f}{J} & 0 \\ 0 & 0 & 1 & 0 \end{bmatrix} . \begin{bmatrix} Id \\ Iq \\ \omega \\ \theta \end{bmatrix} + \begin{bmatrix} \frac{1}{Ls} & 0 & 0 \\ 0 & \frac{1}{Ls} & 0 \\ 0 & 0 & -\frac{Np}{J} \\ 0 & 0 & 0 \end{bmatrix} . \begin{bmatrix} Vd \\ Vq \\ Cr \end{bmatrix} \\ \begin{bmatrix} Id \\ Iq \end{bmatrix} = \begin{bmatrix} 1 & 0 & 0 & 0 \\ 0 & 1 & 0 & 0 \end{bmatrix} . \begin{bmatrix} Id \\ Iq \\ \omega \\ \theta \end{bmatrix} \end{cases} \quad [8.55]$$

The state system is non-linear in $\omega$. In fact, dynamic matrix $A$ contains speed $\omega$, which is a state variable itself. We then use the expression of the Kalman algorithm in discrete form considering that, in a time interval of $T_e$, the speed is slow variable but updated at each moment $k$.

By carrying out discretization in the first order according to Euler, we obtain:

$$X_{k+1} = X_k + Te.f(k, X_k, U_k)$$

with $T_e$ the sampling period. And thus:

$$X_{k+1} = A_k.X_k + B_k.U_k + W_k$$

By adding the state noise random vector, we obtain:

$$\begin{bmatrix} Id_{k+1} \\ Iq_{k+1} \\ \omega_{k+1} \\ \theta_{k+1} \end{bmatrix} = \begin{bmatrix} 1-\frac{Te}{\tau} & Te.\omega_k & 0 & 0 \\ -Te.\omega_k & 1-\frac{Te}{\tau} & -Te.\frac{Ke}{Ls} & 0 \\ 0 & Te.\frac{Np^2.Ke}{J} & 1-Te.\frac{f}{J} & 0 \\ 0 & 0 & Te & 1 \end{bmatrix} . \begin{bmatrix} Id_k \\ Iq_k \\ \omega_k \\ \theta_k \end{bmatrix} + \begin{bmatrix} \frac{Te}{Ls} & 0 & 0 \\ 0 & \frac{Te}{Ls} & 0 \\ 0 & 0 & -Te.\frac{Np}{J} \\ 0 & 0 & 0 \end{bmatrix} . \begin{bmatrix} Vd_k \\ Vq_k \\ Cr_k \end{bmatrix} + W_k \quad [8.56]$$

We should then calculate variables necessary to the implementation of the Kalman algorithm:

$$F_k = \frac{\partial}{\partial X} f \Big|_{\hat{X}_{k|k}}$$

$$= \begin{bmatrix} 1-\frac{Te}{\tau} & Te.\hat{\omega}_{k|k} & Te.\hat{I}q_{k|k} & 0 \\ -Te.\hat{\omega}_{k|k} & 1-\frac{Te}{\tau} & Te.\left(-\hat{I}d_{k|k}-\frac{Ke}{Ls}\right) & 0 \\ 0 & Te.\frac{Np^2.Ke}{J} & 1-Te.\frac{f}{J} & 0 \\ 0 & 0 & Te & 1 \end{bmatrix} \quad [8.57]$$

$$H_k = \frac{\partial}{\partial X} g \Big|_{\hat{X}_{k+1|k}} = C = \begin{bmatrix} 1 & 0 & 0 & 0 \\ 0 & 1 & 0 & 0 \end{bmatrix} \quad [8.58]$$

$$D_k = \frac{\partial}{\partial W} f \Big|_0 = 1 \text{ and } E_k = \frac{\partial}{\partial W} g \Big|_0 = 1 \quad [8.59]$$

In order to implement the Kalman filter in the self-guided synchronous machine, we have to choose the matrix values of initialization $P_0$, state noise $Q_k = Q$, and measurement noise $R_k = R$. This is major in ensuring the correct estimation of position and speed.

### 8.4.4. *Gain adjustment*

The goal of this part is to efficiently adjust the covariance error matrix to initial state and state and measurement noise matrices in order to obtain correct convergence of velocity and measurement estimates with their real values. We should reiterate that these parameters are linked to the variance of random noises difficult to quantify. However, we can ignore the influence of correlation between the different noises as a first simplification and thus have symmetrical matrices defined as positive.

Adjusting matrix factors:

$$P_0 = \begin{bmatrix} e & 0 & 0 & 0 \\ 0 & f & 0 & 0 \\ 0 & 0 & g & 0 \\ 0 & 0 & 0 & h \end{bmatrix} \quad Q = \begin{bmatrix} a & 0 & 0 & 0 \\ 0 & b & 0 & 0 \\ 0 & 0 & c & 0 \\ 0 & 0 & 0 & d \end{bmatrix} \quad R = \begin{bmatrix} i & 0 \\ 0 & j \end{bmatrix}$$

8.4.4.1. *First tests*

As we have noted, the simulation involving a system that is not very noisy compared to a real system, we first chose low adjustment of covariance matrices:

$$P_0 = \begin{bmatrix} 0.01 & 0 & 0 & 0 \\ 0 & 0.01 & 0 & 0 \\ 0 & 0 & 0.01 & 0 \\ 0 & 0 & 0 & 0.01 \end{bmatrix} \quad Q = \begin{bmatrix} 0.01 & 0 & 0 & 0 \\ 0 & 0.01 & 0 & 0 \\ 0 & 0 & 0.01 & 0 \\ 0 & 0 & 0 & 0.01 \end{bmatrix} \quad [8.60]$$

$$R = \begin{bmatrix} 0.01 & 0 \\ 0 & 0.01 \end{bmatrix}$$

Since the machine is initially considered when idle, initial state $X_0$ is zero (in addition, we assume that the error of position at startup is zero). In these conditions and with the rms value of reference current $I_{ref}$ set, the Kalman filter satisfies its role of observation. We can simultaneously see the accurate reconstruction of velocity and position. Position and velocity errors between estimated and real variables are very low (Figure 8.22). We should also note that the signals in fact have very little noise.

For these same $P_0$, $Q$, and $R$ adjustments, we also obtain convergence toward 0 of position and speed errors when current reference $I_{ref}$ is modified. On the other hand, for low currents, the system diverges regardless of $P_0$, $Q$, and $R$ matrices tested. In fact, measurement and state noise matrices should theoretically be sized according to stochastic noises (Figure 8.23). However, weak noises existing in the system mainly come from digital division, so they do not satisfy the characteristics defined previously. The influence of adjustment parameters is highlighted by deteriorating the conditions of simulation:

– by adding random noise in current measurements;

– by having an incorrect position initialization.

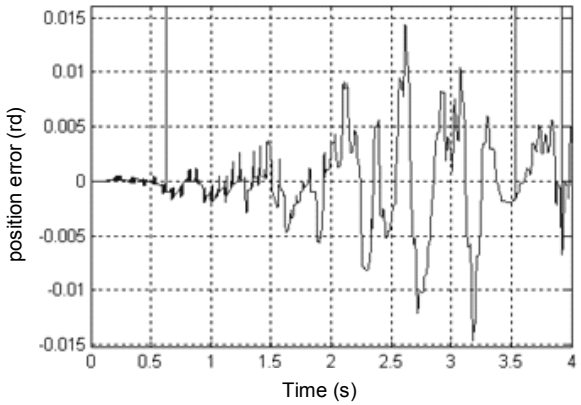


(a)

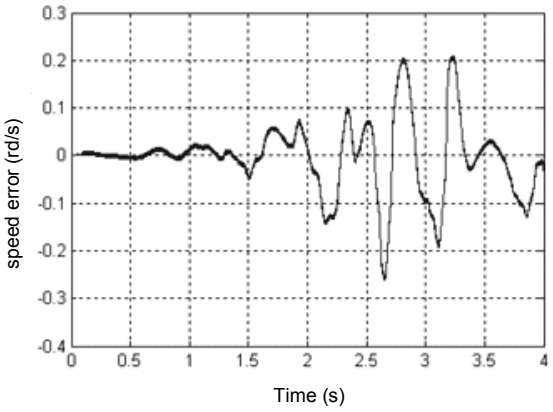


(b)

**Figure 8.22.** *Position and velocity estimation errors*

8.4.4.2. *Addition of Gaussian noise in current measures*

Because of the dynamic chosen for controlling currents, $I_d$ and $I_q$ reach their reference values very quickly (in approximately 0.5 ms in this case). If we focus on the previous currents, where all diagonal terms of adjustment matrices were set at 0.01, and waiting established currents, we have $Id = 0 \pm 0.08A$ and $Iq = -3.45 \pm 0.08A$. If we assimilate these slight current variations to standard deviation $\sigma = 0.08$, the variance is of $v = \sigma^2 = 0.0064$. The choice of variances in the noises of measurement matrix $R$ to 0.01 is therefore coherent.

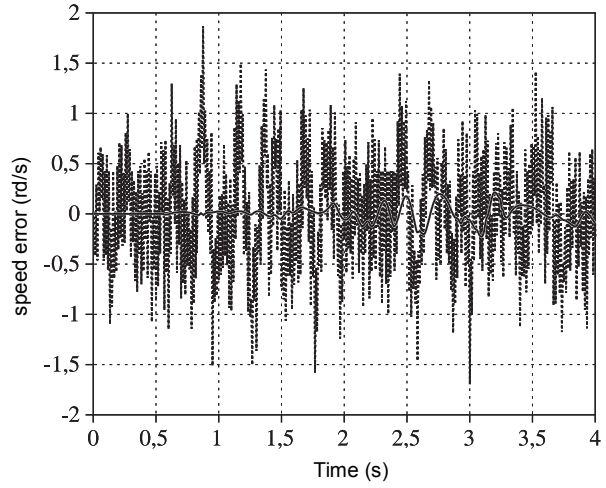


(a)

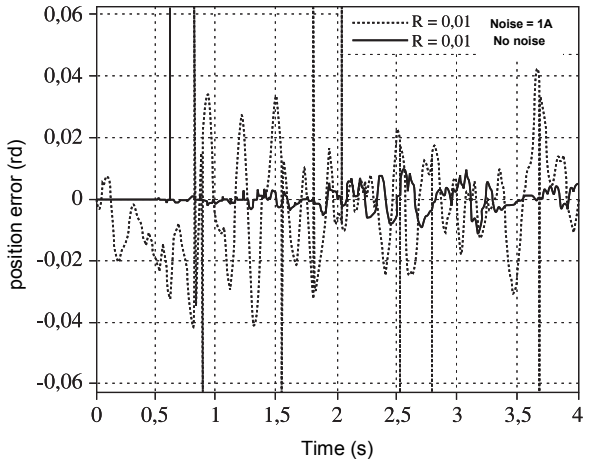


(b)

**Figure 8.23.** *Position and velocity estimation errors*

We will then insert random noise in currents to see the reaction of the observer and to see if the modification of matrix $R$ can overcome this additional noise (Figure 8.24). By adding noise between ±1 A, the observer becomes incorrect. State variables $I_{dkk}$ and $I_{qkk}$ are noisier and deteriorate velocity and position estimations. We then see the importance of identifying measurement noises and corresponding adjustment of matrix $R$.

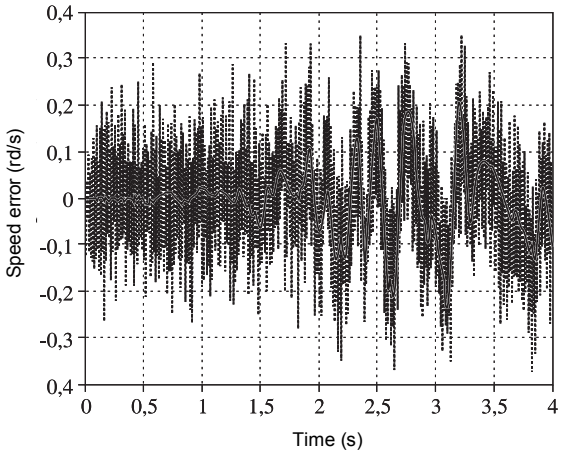


(a)

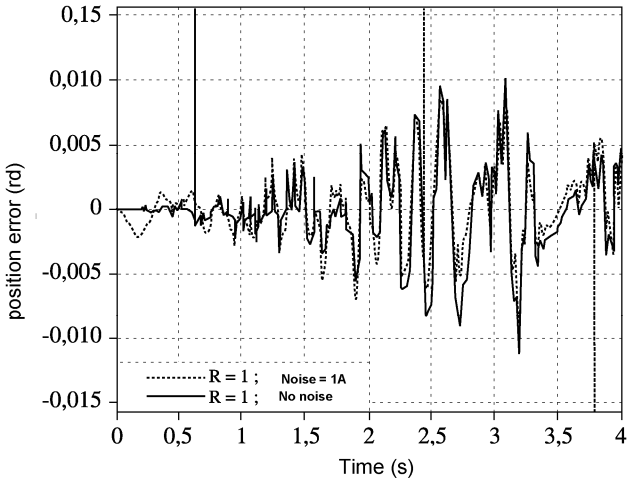


(b)

**Figure 8.24.** *Position and velocity estimation errors: adapted R*

To manage this level of noise, we should adapt the factors of the measurement noise matrix: noise $\approx 1A \Rightarrow \sigma \approx 1 \Rightarrow v = \sigma^2 \approx 1 \Rightarrow$ coefficients of $R = 1$.

We then find the same behavior as before, except that the estimated speed has more noise, but has the same instantaneous mean value as before. In addition, by increasing $R$ ($R$ = 10), we get closer to the initial case. We can then conclude that

diagonal $R$ factors should be set at a minimum value that is equal to the square of the maximum noises observed beforehand. Adjustment factors can be grouped according to the nature of information that they use. In our case, we will apply the same factors on current information ($a = b$, $i = j$, $e = f$) and other weights on the position ($d$, $h$) and velocity ($c$, $g$).

8.4.4.3. *Initial matrix of $P_0$ errors of estimation*

An incorrect estimation, not only at initial moments, can be caused by an incorrect initialization of $P$. We first look for the influence of the covariance terms of initialization $P_0$ matrix. There are two different pieces of information which can be distinguished; the two terms linked to $I_d$, $I_q$, and the terms linked to speed $\omega$ (the term linked to position $\theta$ does not seem to have an influence).

Regardless of the value of the two variance terms linked to currents in $P_0$, there is no visible influence on the convergence of the estimator. In fact, as with both currents, $I_d$ and $I_q$ reach their references in 0.5 ms, the two variance terms associated with matrix $P_{k|k}$ also reach sinusoidal mode at the same time. It is therefore useless to try to initialize these two terms, because at the end of five division periods, they reach a value depending on other variables. On the other hand, the initialization of the factor linked to velocity leads to certain performance modifications. We modify the Kalman gain, and consequently the weighing of measurement coefficients. However, we cannot easily improve the time of convergence of the position. Since the covariance matrix of estimation errors at initial moment has little influence, or for a short period of time, we focus on the matrix of state noise $Q$.

8.4.4.4. *Matrix of state noise Q*

The matrix of state noise $Q$ also has an influence on the covariance matrix of estimation errors $P$. Since $P_0$ makes it easy to set the variance of errors at initial state, the sinusoidal mode reached by $P$ is a function of $Q$. We make the same distinction for the matrix of state noise as for $P_0$. In fact, the coefficients linked to the currents and positions have very little influence. The speed term is the only one significantly modifying the observer behavior.

If we set all the diagonal terms of matrices $P_0$, $Q$, and $R$ at 0.01 and vary the term linked to speed in $Q$ (0.1 or 0.001), we greatly modify the performances of the Kalman filter.

The modification of matrix $Q$ deteriorated the estimation of speed (and position). Figure 8.25 a decrease of $Q$ creates an outburst of speed and position estimates; the machine turns more than it does in reality.

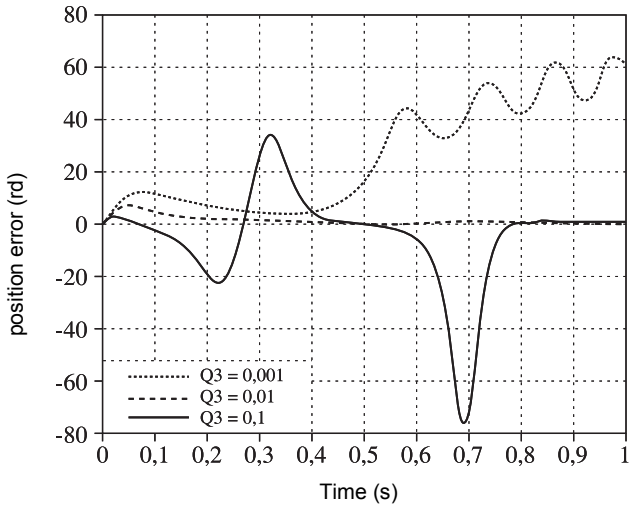


**Figure 8.25.** *Velocity estimation error according to Q*

On the other hand, an increase of $Q$ slows down the estimation; even if the convergence in speed and position is efficient from 0.8 s, a complete rotation was missed and the estimation is therefore incorrect.

Inserting an error of position at startup confirmed the importance of the $Q$ adjustment at state noise level. State noises have their origin in modeling errors of the system and voltage measure (inputs).

By increasing $Q$, we lose information necessary for the correct operation of the estimation. On the other hand, by decreasing $Q$, we take into consideration noises distorting estimation. Unfortunately, the adjustment of $Q$ that is satisfactory for $I_{ref} = 2$ A is no longer suitable for 1 A, so the adjustment of $Q$ should be decreased.

### 8.4.5. *Assessment on the adjustment of Kalman filter factors*

If the coefficients of matrix $Q$ are much greater than those of $R$, the value of corrections $K$ increases quickly and transitory performance is better. That is the case for a device with model uncertainties.

If matrix $R$ is large (significant measurement noises) $K$ is lower and the observation has a hard time converging and mediocre transitory performance.

In addition, if we take large matrix $Q$ (reliable to the model) and very small matrix $R$ (good reliability in measurements), an instability is created because of the measures taken on a device with an incorrect model. The coefficients should be evaluated by a trial and error method in order to adjust them to the device and tolerated performance [VAS 98]. However, methods for understanding these values exist (fuzzy rules, neural network, etc.) or, in this case, the experimental design method can help, to determine the optimal clearance of factors by a minimum number of tests on the real device.

The equations from modeling and their electric and mechanical parameters are therefore very important in obtaining a correct estimation. On the other hand, in reality, these factors also have a lot of errors known with $x$% of accuracy and variable during operation.

We do not use the form of extended Kalman filter for the estimation of parameters that have even larger matrices. In fact, the implementation of a four-dimensional algorithm (as presented) requires a large number of calculations and often creates a problem for the implementation in electrotechnical devices controlled by a small sampling period (200, 100, or even 50 μs) linked to the performance of converters.

## 8.5. Comparison of reconstructions by Kalman filter or analytical redundancy observer

We saw in the previous section that adjustment parameters for the two observers are very different. We will now try to compare them in terms of performance on the basis of rating, initialization error in the rotor position, or an identification error of the machine's electric parameters.

To get different comparison criteria, we use the two observers in the variable speed chain of control of a synchronous machine. This control requires the precise control of currents (using the estimation of the rotor position) and a correct adjustment of current regulators in the converter (PWM) (Figure 8.26).

The speed estimation is used for first generating the speed error for the speed controller.

The control of machine currents needs to be as quick as possible to add velocity control in cascade. We chose a PI regulator for good dynamic response with zero static error.

Without trying to optimize the quality of control, we chose speed regulator gains by compensating the pole for both observers. The mechanical time constant $\tau_\Omega$ was defined at 0.3 s.

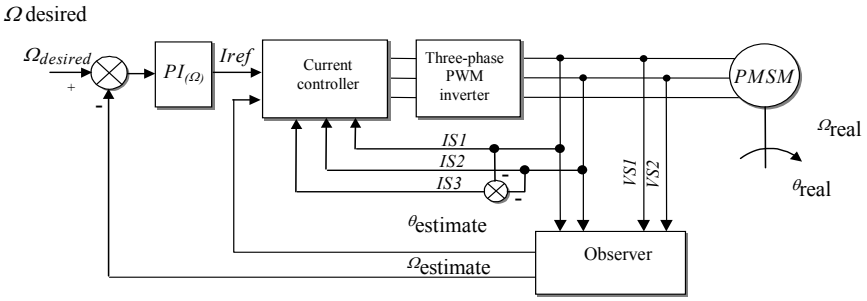


**Figure 8.26.** *Sensorless speed control diagram*

### 8.5.1. *Influence of rating*

At high and average speeds, both observers respond really well and identically. Velocity and position estimations converge rapidly and both systems respond at the same time to speed control.

We should note, however, that the velocity estimate calculated by analytical redundancy is clearly noisier Figure 8.27.

On the other hand, at slow speeds, the analytical redundancy observer is the only one ensuring correct estimation. The Kalman filter works incorrectly. We saw earlier that the Kalman algorithm can diverge for low currents and not work at low speed. Lower levels can also trigger problems in the analytical redundancy observer and would require another adjustment factor case. An adaptation or commutation of factors can therefore be considered (for the two observer structures) [FUR 92]. However, the coefficients used in the redundant observer turn out to be globally satisfying. In fact, other adjustment factors can be defined to improve (not much) low (respectively high) speed performance, but by deteriorating the other case, for a small gain in performance.

We simulated a velocity step of +200 at 0 rad/s. Both algorithms show the same weakness at the machine's stop. In fact, position estimates continue to evolve during a short time, whereas the machine is already stopped. The final position errors are similar for both estimators and exceed one mechanical degree.

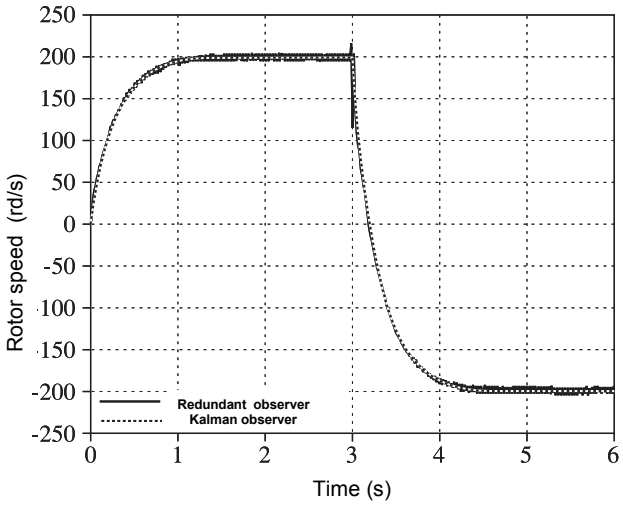


**Figure 8.27.** *Sensorless speed response with a step of* ± 200 *rad/s*

### 8.5.2. *Influence of the initial rotor position*

As seen earlier, the Kalman algorithm is sensitive to an initialization error. What about the analytical redundancy algorithm? Position errors (Figure 8.28) are indicated for an initial mechanical error of 30°. The errors are much better controlled by analytical redundancy than with the Kalman filter. The Kalman algorithm only optimizes the variances of estimation errors and does not accelerate the convergence as the analytical redundancy observer does.

However, the Kalman observer is able to make the estimation successful regardless of the initial error of mechanical angle if the device does not require too much torque at startup (idle machine, etc.). If the angle exceeds 45° mechanical, the redundancy algorithm converges well, but the estimate is completely wrong because the machine starts turning in the other direction from the direction imposed by the current sign.

### 8.5.3. *Sensitivity to electric parameters*

We test the behavior of both algorithms, without exactly knowing the model of the synchronous machine simulated, and evaluate the robustness of observers in relation to an error on stator resistance. The value of this stator resistance evolves according to temperature and we should consider these variations.

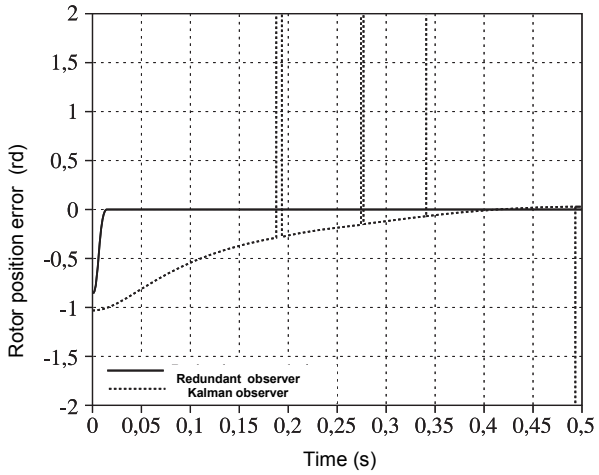


**Figure 8.28.** *Position error of both observer structures*

Assume an error of –25% compared to the real value of $R_s$. The estimation of position (Figure 8.29) is disturbed for both algorithms, but in a lesser measure for analytical redundancy (section 8.4.2). The $R_s$ error is a source of static error, preventing the convergence toward 0. Although the static error for the Kalman filter is approximately 1° mechanical, for the analytical redundancy observer, it is very close to 0°.

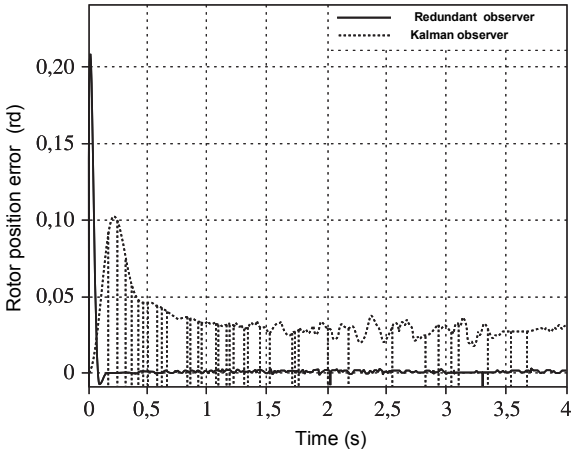


**Figure 8.29.** *Position error with error in resistance $R_s$*

The analytical redundancy algorithm is also more robust than the Kalman filter for other variations of electric parameters, stator inductance $L_s$, or the factor of $K_e$ flux. We do not present results here; these parameters are generally well known.

The analytical redundancy algorithm has an additional advantage: finding information on knowledge errors of $R_s$ and $K_e$ via the corrective term $\Delta\omega_c$ (not in the inductance because the structure loses information linked to $L_s$). We can update the value of these parameters and obtain convergence to 0 of estimates. The calculations are altogether on a different scale to those necessary for the estimation of parameters with the Kalman filter [CAU 05].

The equations of the analytical redundancy algorithm are easier than four-dimensional discrete equations of the Kalman filter. Adjustment factors are in both cases not easy to define and should go through a phase of trial and error with an advantage to the redundancy observer where proportional gain $K_p$ is enough to converge information.

Both algorithms are sensitive to the factors of the system model, with a "simple" correction possibility for the analytical redundancy observation. The volume of calculation to do is quite reduced for the redundancy observer and even if in both cases rotor initial position (or estimation of initial position) is necessary, good performance is obtained for the control of a synchronous actuator without any mechanical sensor.

### 8.5.4. *Influence and management of load torque*

For the convergence of an observer included in a control loop (position, velocity loop), the consideration of the load torque is often necessary. It is often possible to add a load torque estimation in order to increase the quality of the speed, torque, and current response. This estimation is re-injected to obtain a compensation (dealt with in other chapter in this volume). In a sensorless control, a load torque observation can be introduced. This observation is either expressed by an additional state in the Kalman filter, or by a separate observer dedicated to the load torque. There are techniques based on the adaptation of reference models (MRAS, see other chapters).

Control diagram (Figure 8.30) is slightly more complex because of hierarchization. State variables are "independently" observed from the reconstruction of the load torque. The desired dynamics and complexity of algorithms are adapted according to necessary information.

This estimated load torque (Figure 8.31) is used as compensation in order to improve the global actuator performance and obtain torques, currents, and electromotive forces that are less disturbed and easily rebuilt.

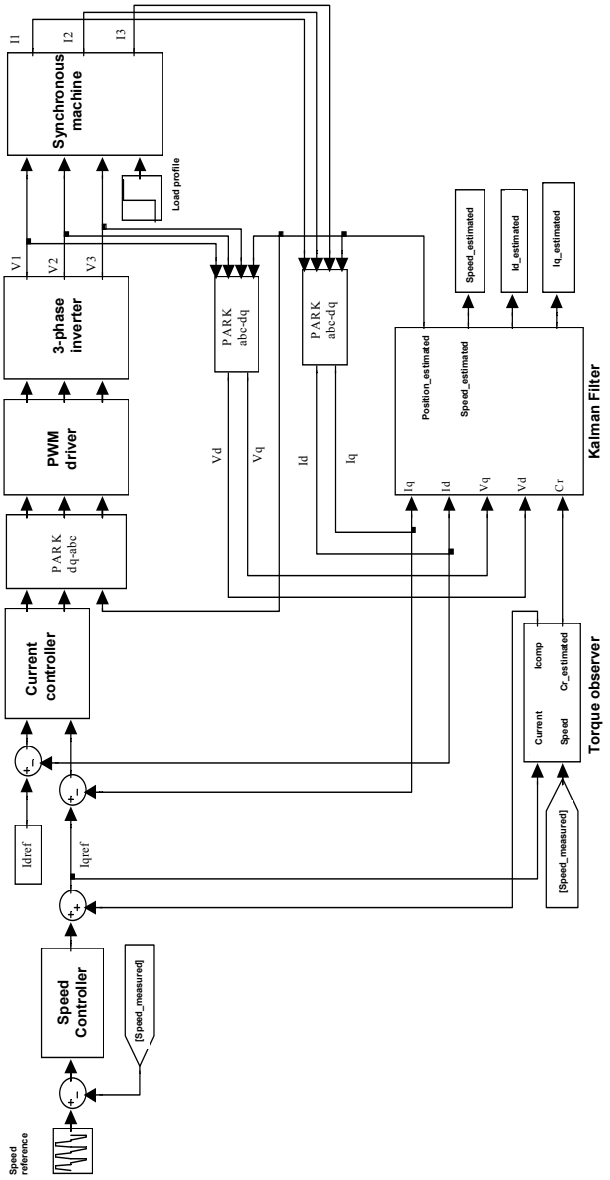


**Figure 8.30.** *Observations of position, speed, and load torque*

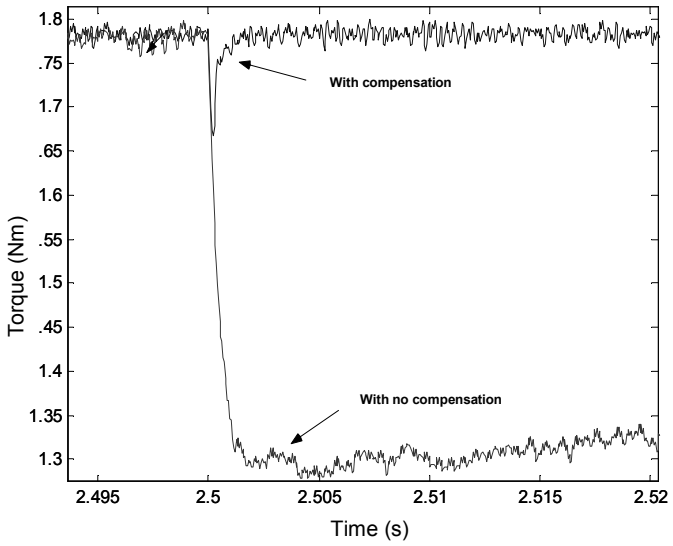


(a)

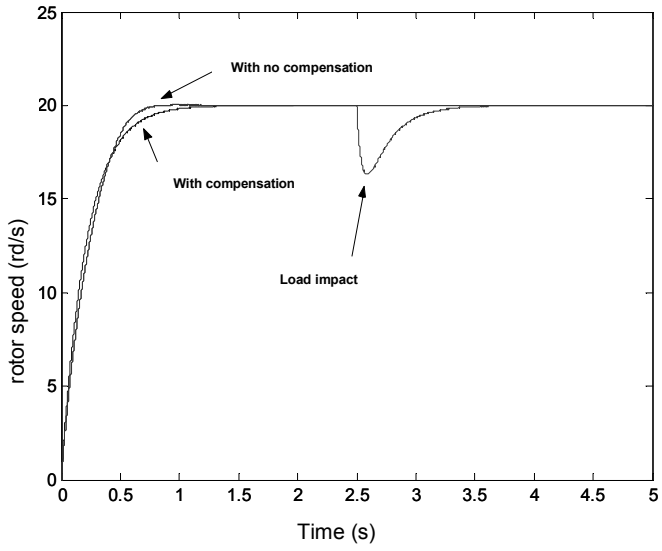


(b)

**Figure 8.31.** *Sensorless torque and velocity response, with and without compensation of estimated load torque*

This control diagram has all the components of the variable speed control of a sensorless synchronous actuator. The voltage inverter operating in Pulse Width Modulation is current-controlled. In fact, the torque control is done by current regulation in axes *d*, *q* ($I_{dref} = 0$ and $I_{qref}$ output of prior regulator).

For each transformation of three-phase/two-phase coordinates, the position estimated is provided by the Kalman filter (the redundancy observer provides the same basic performance).

By using currents and estimated speed, a reduced order observer makes it possible to estimate the load torque and thus the modification of current to use to compensate its effects [TAT 98].

## 8.6. Bibliography

[BOU 06] BOUSSAK M., "Implementation and experimental investigation of sensorless speed control with initial rotor position estimation for interior permanent magnet synchronous motor drive", *IEEE Transactions on Power Electronics*, vol. 20, no. 6, November 2006.

[CAR 90] CARTIGNIES M., Etude de l'autopilotage à partir des tensions d'une machine synchrone alimentée par onduleur de tension (contrôle en courant), Memoir CNAM in Electro-technics – Lajoie-Mazenc M. (ed.), Toulouse, February 1990.

[CAU 02] CAUX S. *et al.*, "Robust development of Matsui's observer", *Proceedings of IECON'02*, Seville, Spain, November 5-8, 2002.

[CAU 05] CAUX S. *et al.*, "Kalman filter and redundant observer comparison for sensorless PMSM velocity control", *Proceedings of International Symposium on Industrial Electronics ISIE05*, Dubrovnik, Croatia, June 2005.

[CAU 06] CAUX S. *et al.*, "Experimental plan design for the tuning of a redundant observer a PMSM drive", *Proceedings of Industrial Electronic Conference, IECON06*, Paris, France, November 7-10, 2006.

[FUR 92] FURUHASHI T. *et al.*, "A position and velocity sensorless control for brushless DC motors using an adaptive sliding mode observer", *IEEE Transaction IES*, vol. 36 no. 3, p. 89-95, 1992.

[GAS 02] GASC L. *et al.*, "Modelling of non sinusoidal permanent magnet synchronous machines with the aim of control", *7th International Conference on Modeling and Simulation of Electric Machines, Converters and Systems, ELECTRIMACS'02*, Montreal, Canada, August 18-21, 2002.

[GRE 95] GRENIER D., LOUIS J.-P., "Modelling for control of non-sine wave permanent-magnet synchronous drives by extending Park's transformation", *Mathematics and computer in Simulation*, vol. 38, no. 4-6, p. 445-452, 1995.

[JEO 03] JEONG Y. *et al.*, "Initial rotor position estimation of an interior permanent magnet synchronous machine using carrier-frequency injection methods", *IEEE Proceedings of International Electrical Machines and Drives Conference*, Madison, June 2003.

[KAL 63] KALMAN R.E., "Mathematical description of linear dynamical systems", *SIAM Journal Control*, vol. 1, p. 152-192, 1963.

[KIM 03] KIM H. *et al.*, "Sensorless control of interior permanent-magnet machine drives with zero-phase lag position estimation", *Transaction on Industry Application*, vol. 39 no. 6, p. 1726-1733, November/December 2003.

[MAT 96] MATSUI N., "Sensorless PM brushless DC motor drives", *IEEE Transaction on Industrial Electronics*, vol. 43 no. 2, p. 300-308, April 1996.

[MOB 00] MOBARAKEH B. *et al.*, "A globally converging observer of mechanical variables for sensorless PMSM", *Proceedings of PESC'2000*, Galway, Ireland, June 2000.

[PEY 03] PEYRAS L., Observateurs de position pour la machine synchrone avec prise en compte d'incertitudes paramétriques, Doctoral Thesis, no. 2019, INP, Toulouse, 2003.

[SCH 03] SCHROEDL M., "Sensorless control of permanent magnet synchronous machines: an overview", *EPE'2003*, Toulouse, 2003.

[SIC 97] SICOT L., Contribution à l'introduction de limitations dans les lois de commande de la machine synchrone à aimants permanents: approche théorique et réalisations expérimentales – Commande sans capteur, Doctoral Thesis, Nantes, 1997.

[TAT 98] Tatematsu K. *et al.*, "Sensorless control for PMSM with reduced order observer", *Proceedings of PESC'98*, vol. 1, p. 125-131, Charleston, United States, May 1998.

[VAS 01] VAS P. *et al.*, "Sensorless drives, state-of-the art", *Proceedings of PCIM 2001*, Nurenberg, Germany, 2001.

[VAS 98] VAS P., *Sensorless Vector and Direct Torque Control*, Oxford Science Publications, Oxford University Press, 1998.